Emisja klastrów z ciężkich jąder jako bardzo asymetryczne rozszczepienie

M. Warda
UMCS, Lublin

L.M. Robledo, UAM, Madryt

Warszawa, 22-10-2008

Plan:

- Wprowadzenie historyczne i doświadzalne

Plan:

- Wprowadzenie historyczne i doświadzalne
- Szczegóły obliczeń

Plan:

- Wprowadzenie historyczne i doświadzalne
- Szczegóły obliczeń
- ^{234}U - emiter klastrów o średniej masie

Plan:

- Wprowadzenie historyczne i doświadzalne
- Szczegóły obliczeń
- ^{234}U - emiter klastrów o średniej masie
- ^{226}Ra - lekki emiter

Plan:

- Wprowadzenie historyczne i doświadzalne
- Szczegóły obliczeń
- ^{234}U - emiter klastrów o średniej masie
- ^{226}Ra - lekki emiter
- ^{242}Cm - najcięższy emiter

Plan:

- Wprowadzenie historyczne i doświadzalne
- Szczegóły obliczeń
- ^{234}U - emiter klastrów o średniej masie
- ^{226}Ra - lekki emiter
- ^{242}Cm - najcięższy emiter
- Czasy życia

Plan:

- Wprowadzenie historyczne i doświadzalne
- Szczegóły obliczeń
- ^{234}U - emiter klastrów o średniej masie
- ^{226}Ra - lekki emiter
- ^{242}Cm - najcięższy emiter
- Czasy życia
- Podsumowanie

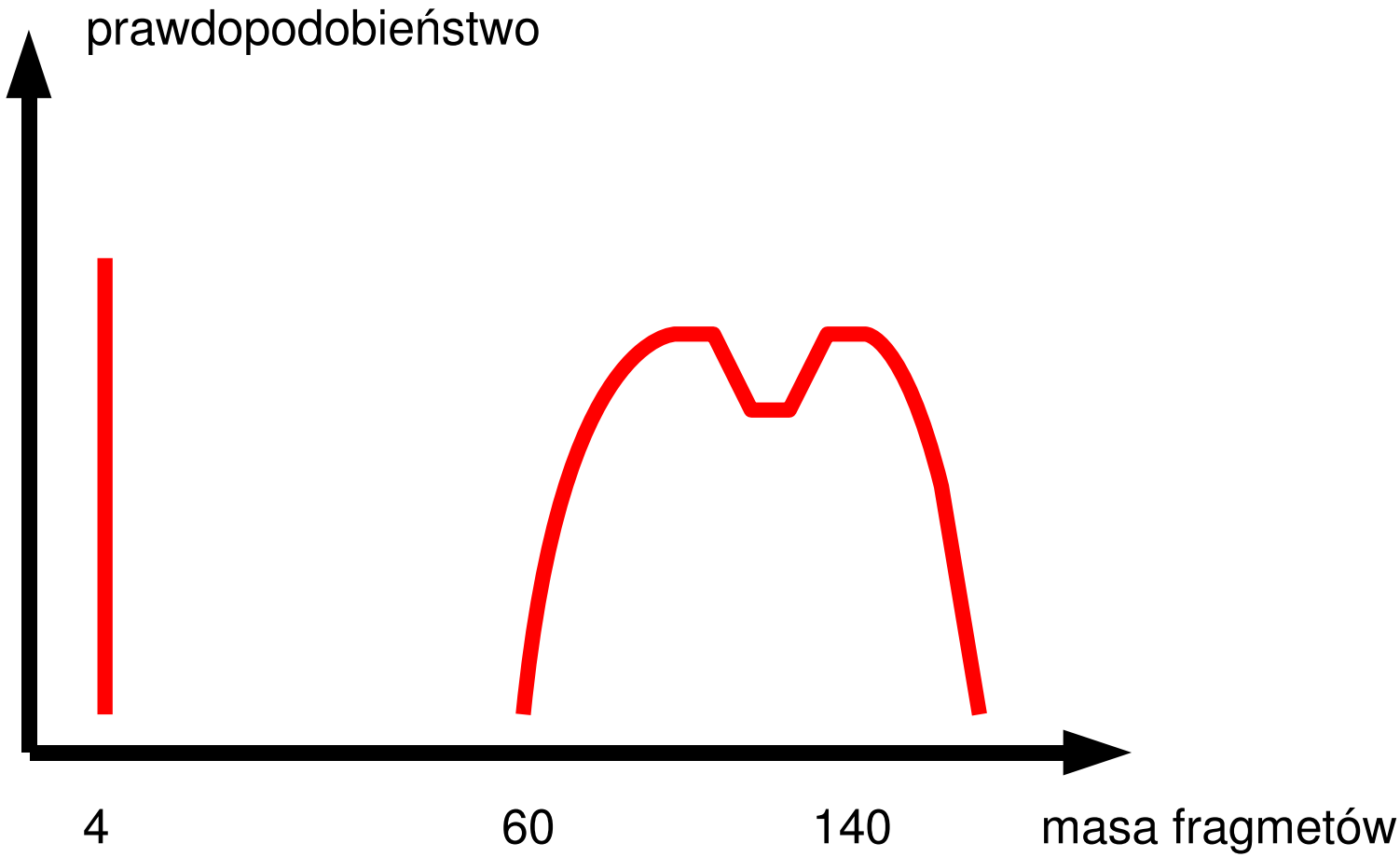
prawdopodobieństwo
4
60
140
masa fragmetów

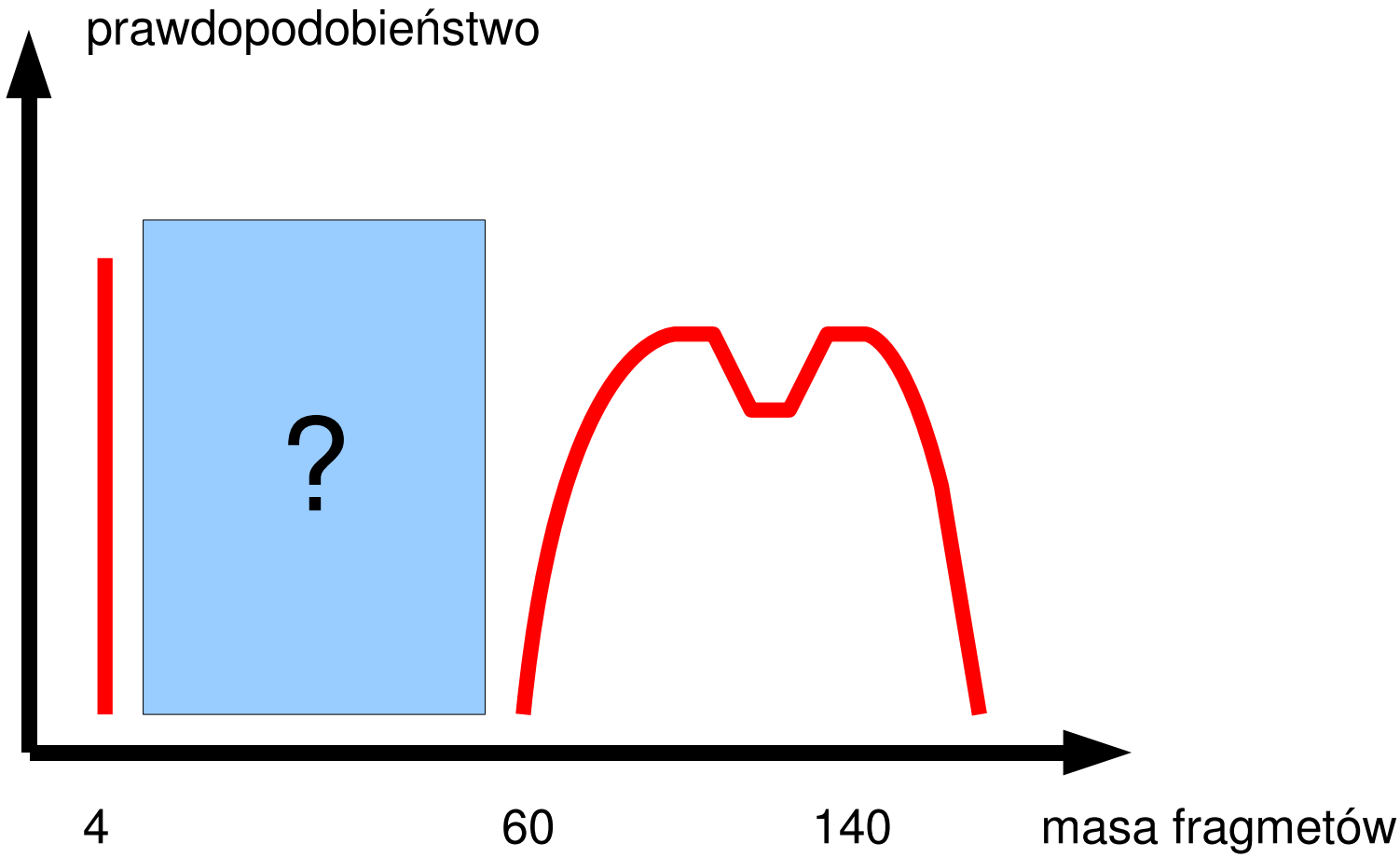
prawdopodobieństwo
?
4
60
140
masa fragmetów

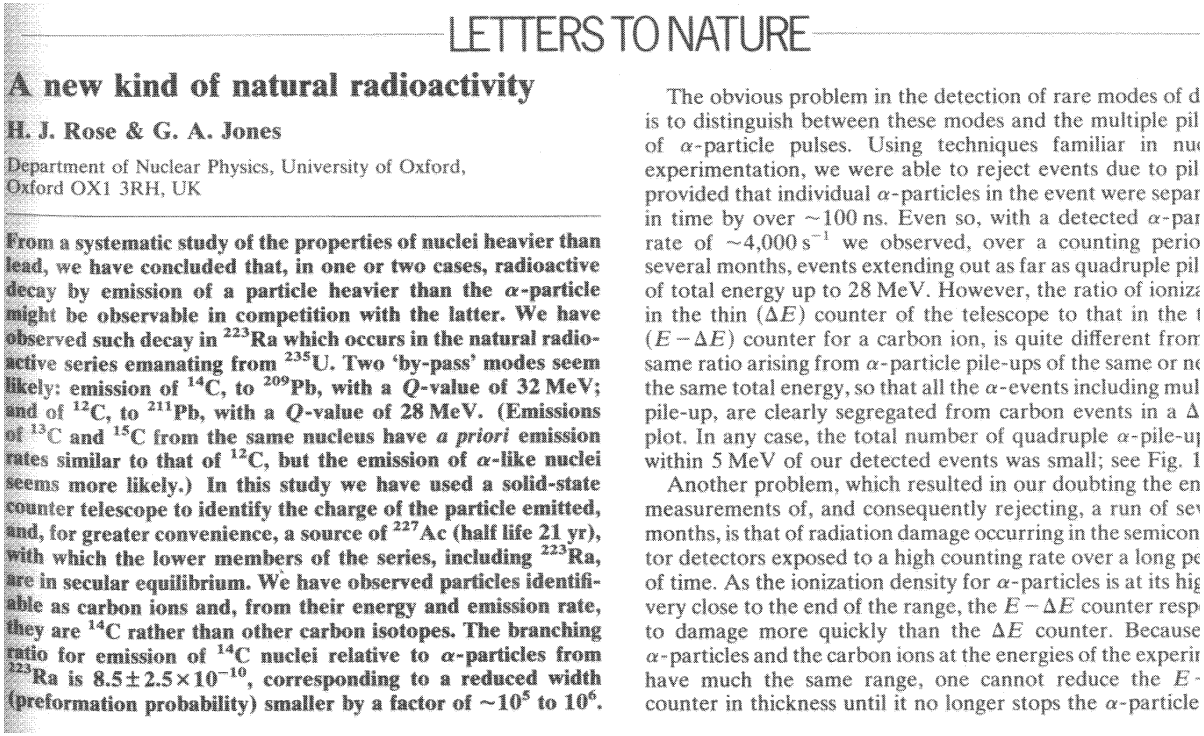

LETTERS TO NATURE

A new kind of natural radioactivity

H. J. Rose & G. A. Jones

Department of Nuclear Physics, University of Oxford, Oxford OX1 3RH, UK

From a systematic study of the properties of nuclei heavier than lead, we have concluded that, in one or two cases, radioactive decay by emission of a particle heavier than the α-particle might be observable in competition with the latter. We have observed such decay in ^{223}Ra which occurs in the natural radioactive series emanating from ^{235}U. Two 'by-pass' modes seem likely: emission of ^{14}C, to ^{209}Pb, with a Q-value of 32 MeV; and of ^{12}C, to ^{211}Pb, with a Q-value of 28 MeV. (Emissions of ^{13}C and ^{15}C from the same nucleus have *a priori* emission rates similar to that of ^{12}C, but the emission of α-like nuclei seems more likely.) In this study we have used a solid-state counter telescope to identify the charge of the particle emitted, and, for greater convenience, a source of ^{227}Ac (half life 21 yr), with which the lower members of the series, including ^{223}Ra, are in secular equilibrium. We have observed particles identifiable as carbon ions and, from their energy and emission rate, they are ^{14}C rather than other carbon isotopes. The branching ratio for emission of ^{14}C nuclei relative to α-particles from ^{223}Ra is $8.5 \pm 2.5 \times 10^{-10}$, corresponding to a reduced width (preformation probability) smaller by a factor of $\sim 10^5$ to 10^6.

The obvious problem in the detection of rare modes of d is to distinguish between these modes and the multiple pil of α-particle pulses. Using techniques familiar in nu experimentation, we were able to reject events due to pil provided that individual α-particles in the event were separ in time by over $\sim$100 ns. Even so, with a detected α-par rate of $\sim$4,000 s^{-1} we observed, over a counting perio several months, events extending out as far as quadruple pil of total energy up to 28 MeV. However, the ratio of ioniz in the thin (ΔE) counter of the telescope to that in the t ($E - \Delta E$) counter for a carbon ion, is quite different from same ratio arising from α-particle pile-ups of the same or n the same total energy, so that all the α-events including mul pile-up, are clearly segregated from carbon events in a Δ plot. In any case, the total number of quadruple α-pile-u within 5 MeV of our detected events was small; see Fig. 1

Another problem, which resulted in our doubting the en measurements of, and consequently rejecting, a run of se months, is that of radiation damage occurring in the semicon tor detectors exposed to a high counting rate over a long pe of time. As the ionization density for α-particles is at its hig very close to the end of the range, the $E - \Delta E$ counter resp to damage more quickly than the ΔE counter. Because α-particles and the carbon ions at the energies of the experi have much the same range, one cannot reduce the E counter in thickness until it no longer stops the α-particle

Rose and Jones, *Nature* **307**, 245 (1984)

$$^{223}_{88}\mathrm{Ra} \longrightarrow {}^{14}\mathrm{C} + {}^{209}\mathrm{Pb}$$

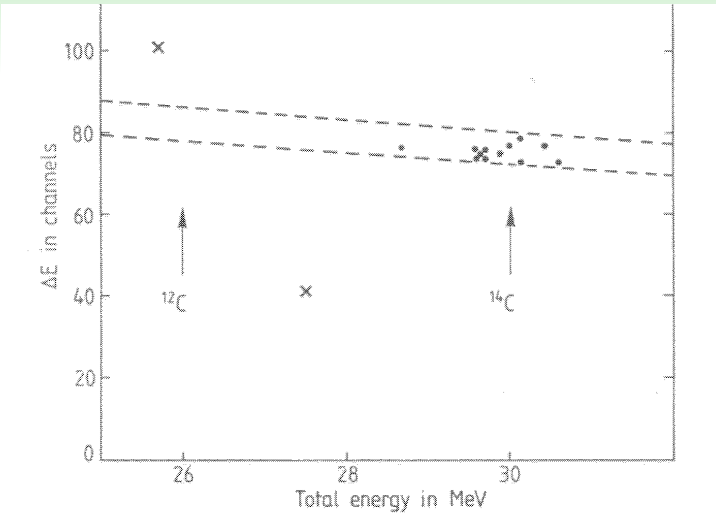

Fig. 1 Contents of the two-dimensional array ΔE versus E_{total} after a run of 189 days. The dotted line indicates the allowed region for carbon ions and the arrows indicate the total energies expected for ^{12}C and ^{14}C emissions in the decay of ^{223}Ra. The lower of the two crosses represents a quadruple pile-up. Below the total energy displayed, large numbers of triple and double α-pile-ups were recorded. Single α-events (and, in part, even double α-pile-ups) were biased out on the analogue side to avoid deadtime problems on the digital side. The upper cross is an event which was recorded during a thunderstorm which affected the mains badly. A run of 194 days was made before this one, yielding 8 events and, in addition, a run of approximately half a year was performed to investigate possible cosmic ray-induced events. Channel 77 in $\Delta E \equiv 6.7$ MeV, which is exactly as expected for 30 MeV ^{14}C. Detector characteristics: The dead layer of the ΔE detector (200 mm^2 active area, 8.2 μm sensitive thickness) was determined to lie between 0.3 and 0.8 μm. In addition a protective layer of gold of thickness 20 $\mu g\,cm^{-2}$ was evaporated on the source and 15 $\mu g\,cm^{-2}$ carbon film inserted between the source and the ΔE detector. An extra 30–40 $\mu g\,cm^{-2}$ of gold is present on the E-detector (300 mm^2 active area). This gives a total of 150–250 $\mu g\,cm^{-2}$ of effective dead layer (Si equivalent) and an energy loss of ^{14}C ions of 0.5–0.8 MeV. The source of strength 3.3 μCi gave a counting rate of $\approx$4,000 s^{-1}, corresponding to an effective solid angle of detection of $\approx 1/3$ sr.

New type of decay of heavy nuclei intermediate betwee fission and α decay

A. Săndulescu and D. N. Poenaru

Institute of Physics and Nuclear Technology, Bucharest

W. Greiner

Institute of Theoretical Physics, J. W. Goethe University, Frankfurt am Main

Fiz. Elem. Chastits At. Yadra **11**, 1334–1368 (November–December 1980)

A new type of decay intermediate between fission and α decay is predicted in heavy and superheavy nuclei. Two limiting approaches are presented in which this decay is treated as fission with maximal asymmetry of the fragment masses or as emission of a heavy cluster. It is shown that, if strongly mass-asymmetric two-body fragmentation is treated as emission of a heavy cluster, agreement is achieved with the predictions made earlier of a strongly asymmetric type of fission representing a new decay mode intermediate between α decay and fission. It is also shown that α decay can be successfully regarded as a fission process with different charge densities of the two fragments and a precisely determined mass ratio.

PACS numbers: 23.90. + w, 23.60. + e, 24.75. + i

Sandulescu, Poenaru and Greiner, *Sov. J. Part Nucl.* **11**, 528 (1980)

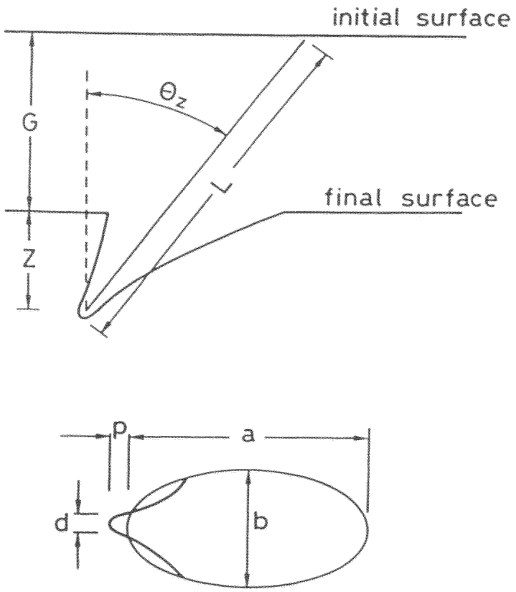

Fig. 1. Geometry of a track etched until the end of the particle range, L. G is the thickness of the material etched away, d the tip diameter, a and b the major and minor axes, p the overhang, Θ_z the zenith angle, z the track depth.

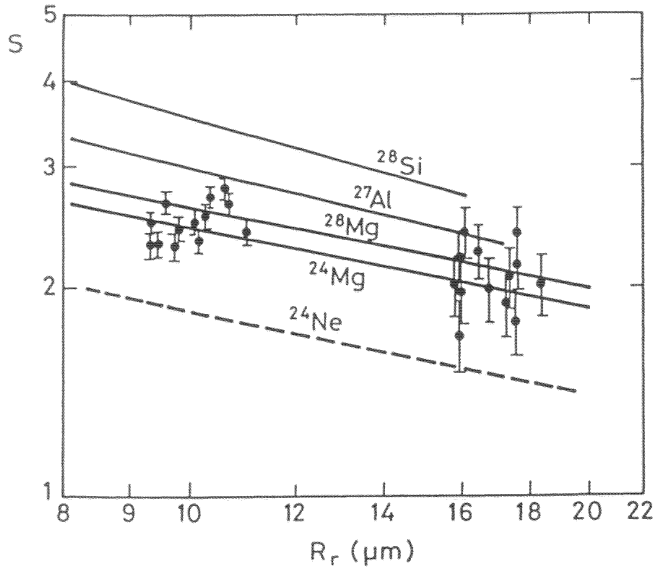

Fig. 6. Comparison of the sensitivity S measured at two stages of the etching process for the 15 events from the decay of ^{236}Pu with accelerator calibrations. Reprinted with permission from M. Hussonnois et al., "Cluster decay of ^{236}Pu and correlations of the probabilities of α decay, cluster decay and spontaneous fission of heavy nuclei" JETP Letters 62 (1995) p 701. Copyright 1995 American Institute of Physics.

R. Bonetti, A. Guglielmetti, in *Heavy Elements and Related New Phenomena Vol II, ed. W. Greiner and R.K. Gupta*, p.634, Word Scientific, 1999

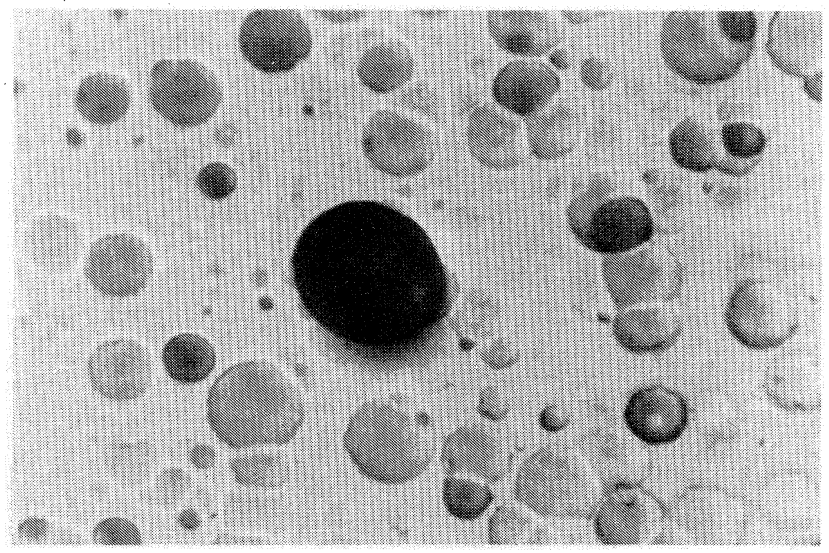

FIG. 1. Photomicrograph showing one etch pit due to a 56 MeV ^{24}Ne ion striking a Cronar detector nearly head on. About 3×10^6 alpha particles passed through this field of view.

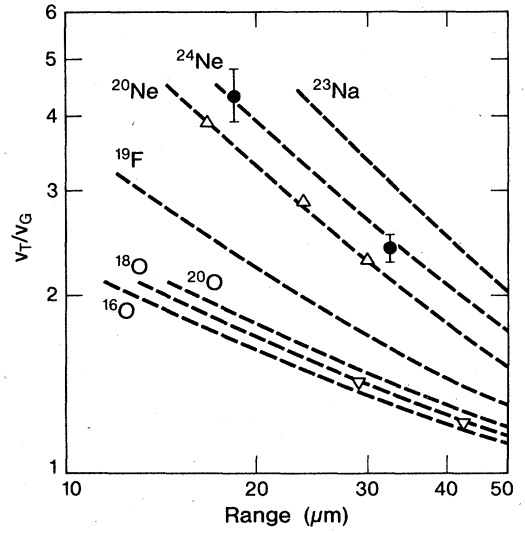

FIG. 2. Comparison of average signal of ^{24}Ne nuclei (●) emitted from ^{232}U with calibrations (dashed lines) obtained with ^{18}O (▽) and ^{20}Ne (△) ions at Lawrence Berkeley Laboratory accelerators. Ratio of etching rate along track to general etching rate v_T/v_G, is plotted as a function of residual range.

Barwick et al., PRC **31**, 1984 (1985)

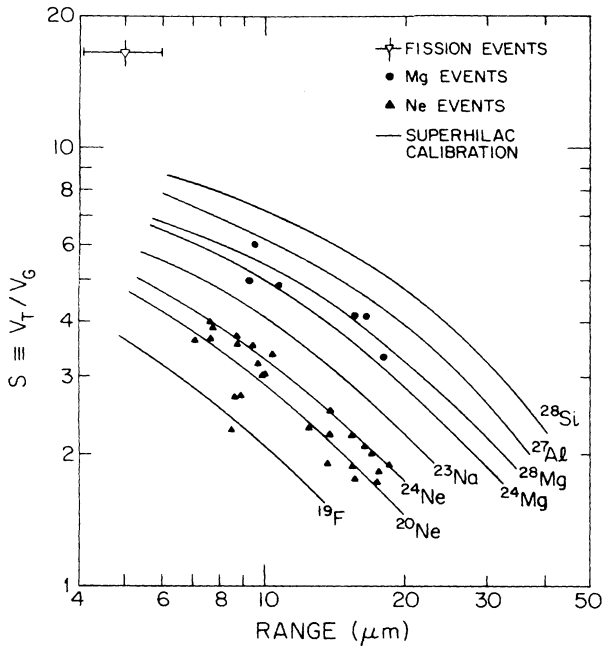

FIG. 1. Identification of ions emitted from ^{234}U as Ne and Mg. The curves are based on calibrations obtained with ^{28}Si, ^{24}Mg, and ^{20}Ne ions at Lawrence Berkeley Laboratory SuperHilac.

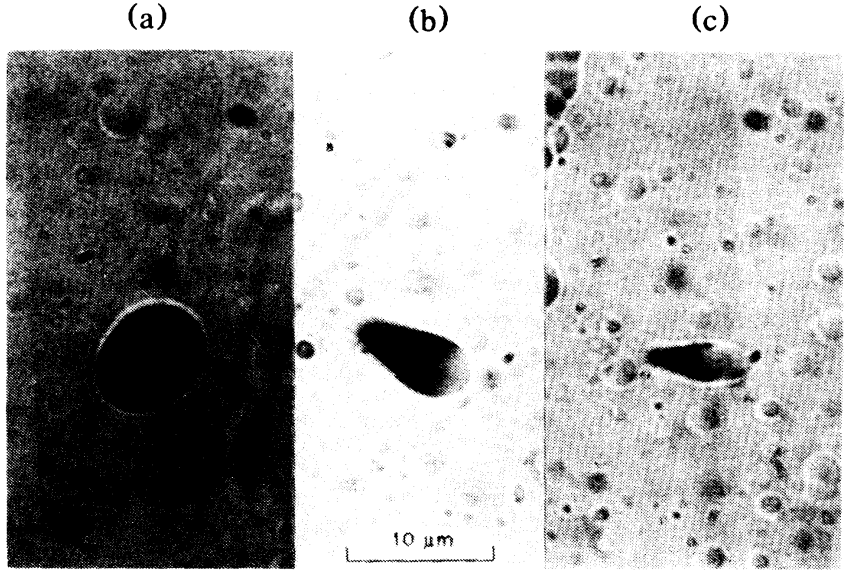

FIG. 2. Photomicrographs showing etch pits due to (a) spontaneous fission, (b) Mg emission, and (c) Ne emission from ^{234}U source.

Wang et al., PRC **36**, 2717 (1987)

$$\log_{10} T_{1/2}^{AZ} = \frac{aA_2\eta + bZ_2\eta_z}{\sqrt{Q}} + c.$$

$a = 10.603$, $b = 78.027$, and $c = -80.66$

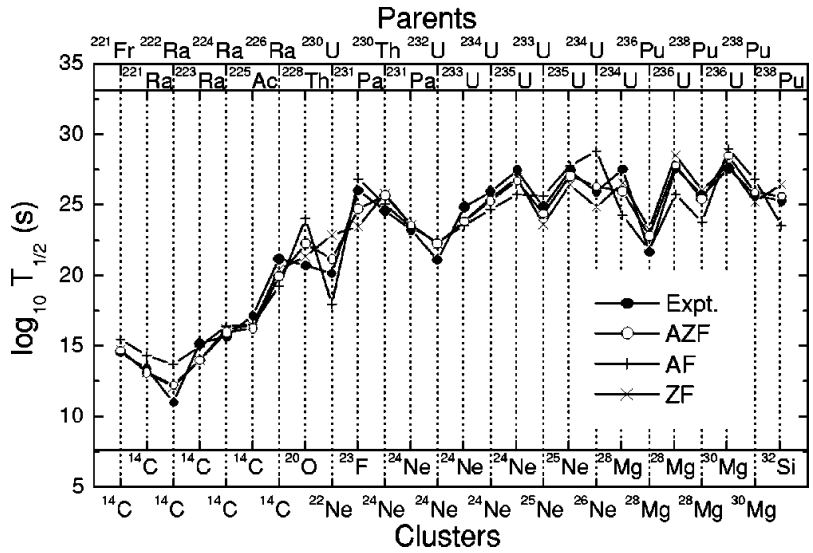

FIG. 1. $\log_{10} T_{1/2}$ (s) for different clusters emitted from various radioactive parents, calculated by using the AZ formula (AZF) and compared with experimental data. Also, the results of calculations for AF ($b=0$) and ZF ($a=0$) truncations of AZF are shown for comparisons.

Balasubramaniam et al., PRC **70**, 017301 (2004)

$$\log_{10} T_{1/2} = a\sqrt{\mu} Z_c Z_d Q^{-1/2} + b\sqrt{\mu}(Z_c Z_d)^{1/2} +$$

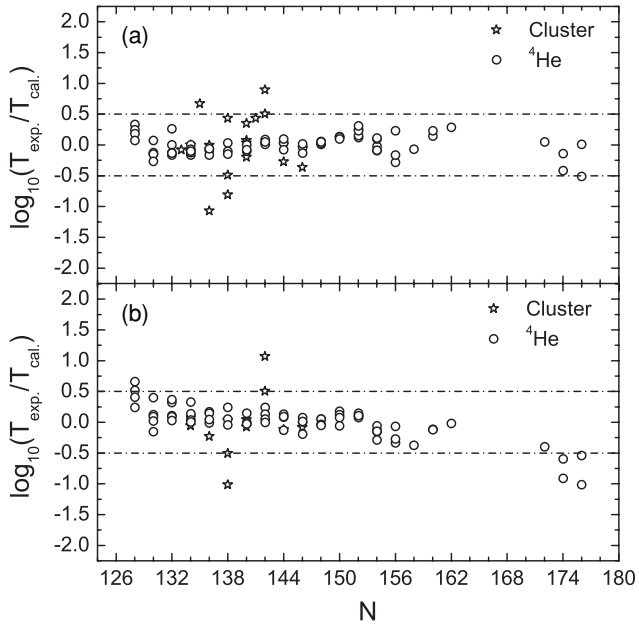

FIG. 4. Deviations between the logarithms of the experimental data and of the calculated values for even-even nuclei (a) when we use two sets of parameters to describe α decay and cluster radioactivity respectively and (b) when we use one set of parameters to describe both α decay and cluster radioactivity at the same time.

Ni et al., PRC **78**, 044310 (2008)

Emisja klastrów

Emisja klastrów

- Emitery: $^{221}_{87}\mathrm{Fr}$ — $^{242}_{96}\mathrm{Cm}$

Emisja klastrów

- Emitery: $^{221}_{87}\mathrm{Fr}$ — $^{242}_{96}\mathrm{Cm}$
- Klastry: $^{14}\mathrm{C}$ — $^{34}\mathrm{Si}$

Emisja klastrów

- Emitery: $^{221}_{87}\mathrm{Fr}$ — $^{242}_{96}\mathrm{Cm}$
- Klastry: $^{14}\mathrm{C}$ — $^{34}\mathrm{Si}$
- Ciężkie fragmenty: $^{208}\mathrm{Pb}$ ± 4 nucleony

Emisja klastrów

- Emitery: $^{221}_{87}\mathrm{Fr}$ — $^{242}_{96}\mathrm{Cm}$
- Klastry: $^{14}\mathrm{C}$ — $^{34}\mathrm{Si}$
- Ciężkie fragmenty: $^{208}\mathrm{Pb}$ ± 4 nucleony
- Czasy życia: 10^{9} — 10^{28} s

Emisja klastrów

- Emitery: $^{221}_{87}\mathrm{Fr}$ — $^{242}_{96}\mathrm{Cm}$
- Klastry: $^{14}\mathrm{C}$ — $^{34}\mathrm{Si}$
- Ciężkie fragmenty: $^{208}\mathrm{Pb}$ ± 4 nucleony
- Czasy życia: 10^{9} — 10^{28} s
- α "branching ratio": 10^{-10} — 10^{-17} s

Szczegóły obliczeń

- Model Hartree-Focka-Bogolubova z siłami Gogny D1S.

Szczegóły obliczeń

- Model Hartree-Focka-Bogolubova z siłami Gogny D1S.
- Obliczenia samozgodne.

Szczegóły obliczeń

- Model Hartree-Focka-Bogolubova z siłami Gogny D1S.
- Obliczenia samozgodne.
- Analiza powierzchni energii potencjalnej z więzami na moment kwadrupolowy i oktupolowy.

Szczegóły obliczeń

- Czasy życia:

$$t_{1/2} = 2.86\,10^{-21}(1 + \exp(2S))$$

Szczegóły obliczeń

- Czasy życia:

$$t_{1/2} = 2.86\,10^{-21}(1 + \exp(2S))$$

- Działanie:

$$S = \int_a^b dq_3 \sqrt{2B(q_3)(V(q_3) - E_0)}$$

Szczegóły obliczeń

- Czasy życia:

$$t_{1/2} = 2.86\,10^{-21}(1 + \exp(2S))$$

- Działanie:

$$S = \int_a^b dq_3 \sqrt{2B(q_3)(V(q_3) - E_0)}$$

- Kolektywny parametr bezwładności:

$$B_{\mathrm{ATDHFB}}(q_3) = \frac{M_{-3}(q_3)}{M_{-1}^2(q_3)}$$

$$M_{-n}(q_3) = \sum_{\mu\nu} \frac{\left|\left(Q_{30}^{20}\right)_{\mu\nu}\right|^2}{(E_\mu + E_\nu)^n}$$

Szczegóły obliczeń

- Czasy życia:

$$t_{1/2} = 2.86\,10^{-21}(1 + \exp(2S))$$

- Działanie:

$$S = \int_a^b dq_3 \sqrt{2B(q_3)(V(q_3) - E_0)}$$

- Kolektywny parametr bezwładności:

$$B_{\mathrm{ATDHFB}}(q_3) = \frac{M_{-3}(q_3)}{M_{-1}^2(q_3)}$$

$$M_{-n}(q_3) = \sum_{\mu\nu} \frac{\left|\left(Q_{30}^{20}\right)_{\mu\nu}\right|^2}{(E_\mu + E_\nu)^n}$$

- "Zero point energy" w stanie podstawowym:

$$E_0 = 0.5\mathrm{MeV}$$

Szczegóły obliczeń

- Energia potencjalna:

$$V(q_3) = V_{HFB}(q_3) - V_{REC}(q_3) - \epsilon_0(q_3)$$

Szczegóły obliczeń

- Energia potencjalna:

$$V(q_3) = V_{HFB}(q_3) - V_{REC}(q_3) - \epsilon_0(q_3)$$

- Energia rotacyjna:

$$V_{REC}(q_3) = \langle \Delta \vec{J}^2 \rangle / (2\mathcal{J}_Y)$$

Szczegóły obliczeń

- Energia potencjalna:

$$V(q_3) = V_{HFB}(q_3) - V_{REC}(q_3) - \epsilon_0(q_3)$$

- Energia rotacyjna:

$$V_{REC}(q_3) = \langle \Delta \vec{J}^2 \rangle / (2\mathcal{J}_Y)$$

- "Zero point energy" :

$$\epsilon_0(q_3) = \frac{1}{2} G(q_3) B^{-1}_{\mathrm{ATDHFB}}(q_3)$$

$$G(q_3) = \frac{M_{-2}(q_3)}{2M^2_{-1}(q_3)}$$

Szczegóły obliczeń

- Energia potencjalna po rozpadzie:

$$V_{two\_fragments}(q_3) = BE_{HFB} - Q + V_{Coul}(q_3)$$

Szczegóły obliczeń

- Energia potencjalna po rozpadzie:

$$V_{two\_fragments}(q_3) = BE_{HFB} - Q + V_{Coul}(q_3)$$

- Energia kulombowska:

$$V_{Coul}(q_3) = e^2 \frac{Z_1 Z_2}{R(q_3)}$$

$$q_3 = f_3 R^3$$

$$f_3 = \frac{A_1 A_2}{A} \frac{(A_1 - A_2)}{A}$$

Szczegóły obliczeń

- Energia potencjalna po rozpadzie:

$$V_{two\_fragments}(q_3) = BE_{HFB} - Q + V_{Coul}(q_3)$$

- Energia kulombowska:

$$V_{Coul}(q_3) = e^2 \frac{Z_1 Z_2}{R(q_3)}$$

$$q_3 = f_3 R^3$$

$$f_3 = \frac{A_1 A_2}{A} \frac{(A_1 - A_2)}{A}$$

- Parametr bezwładności:

$$B(q_3) = \frac{\mu}{9 q_3^{4/3} f_3^{2/3}}$$

$$\mu = m_n \frac{A_1 A_2}{A_1 + A_2}$$

Ścieżka emisji klastru: $^{234}_{92}$U

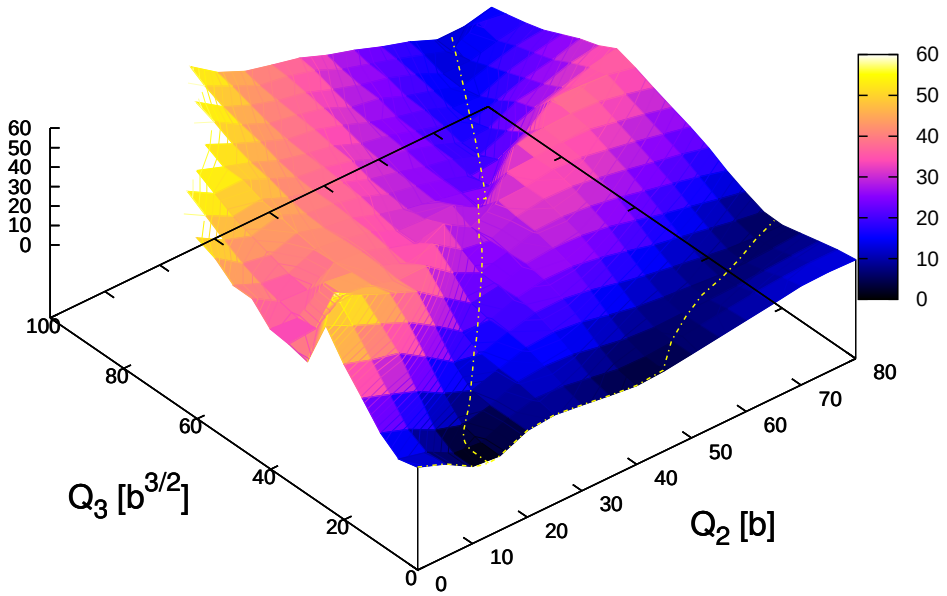

Ścieżka emisji klastru: $^{234}_{92}$U

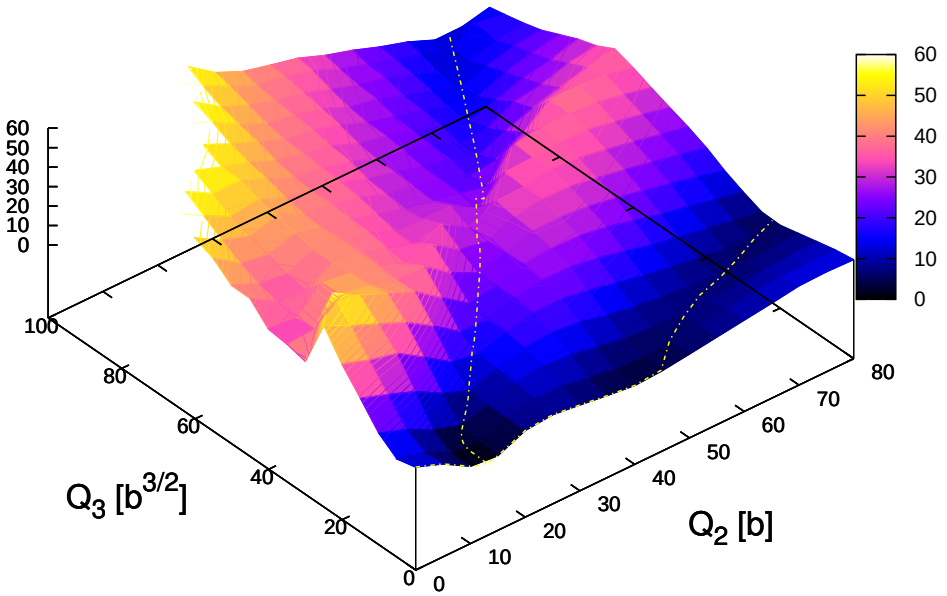

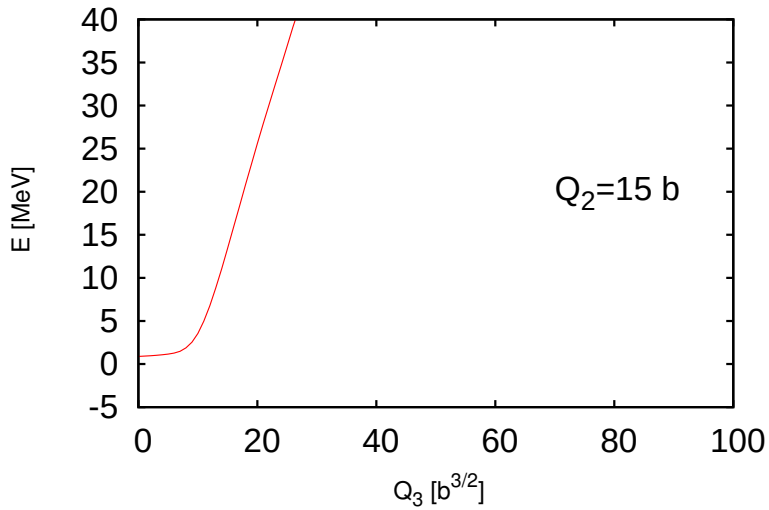

Ścieżka emisji klastru: $^{234}_{92}$U

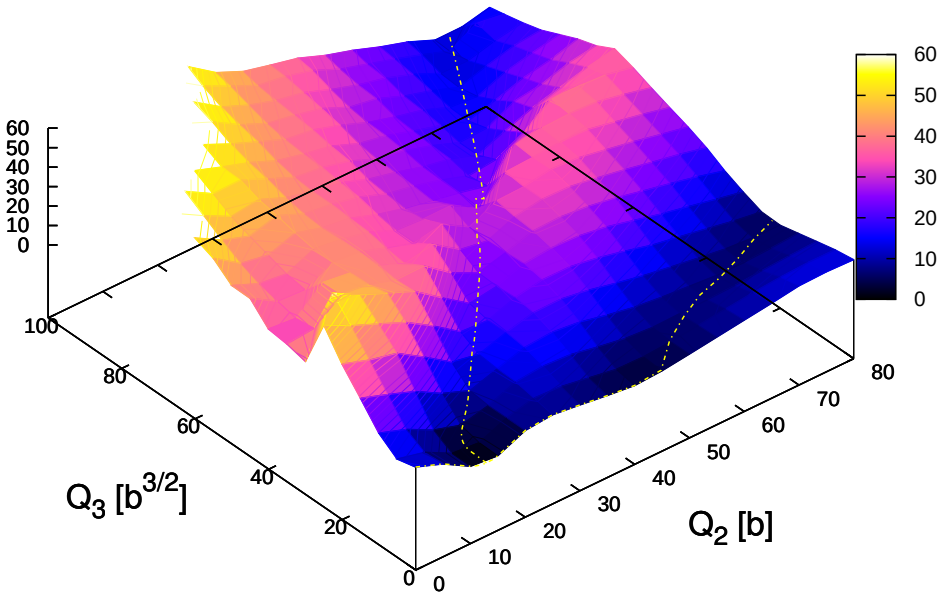

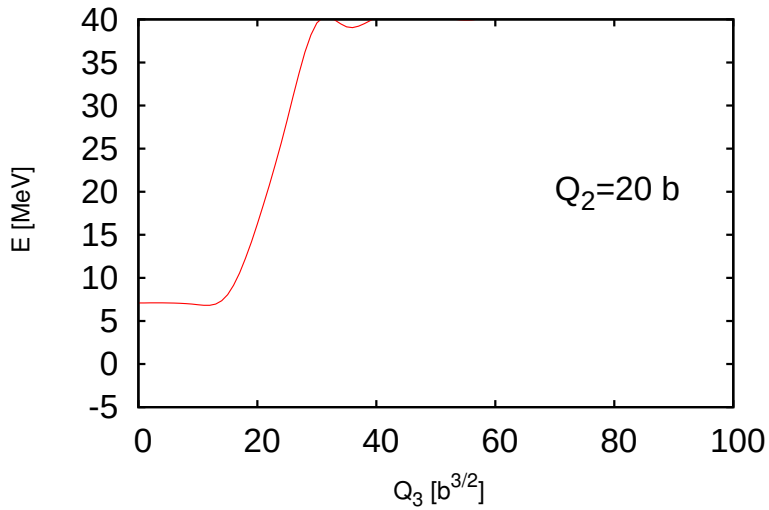

Ścieżka emisji klastru: $^{234}_{92}U$

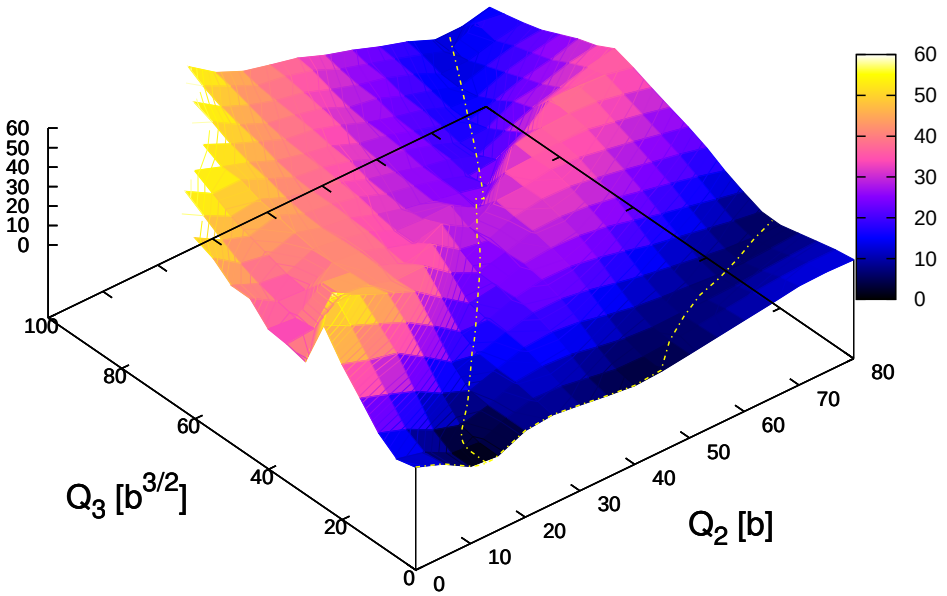

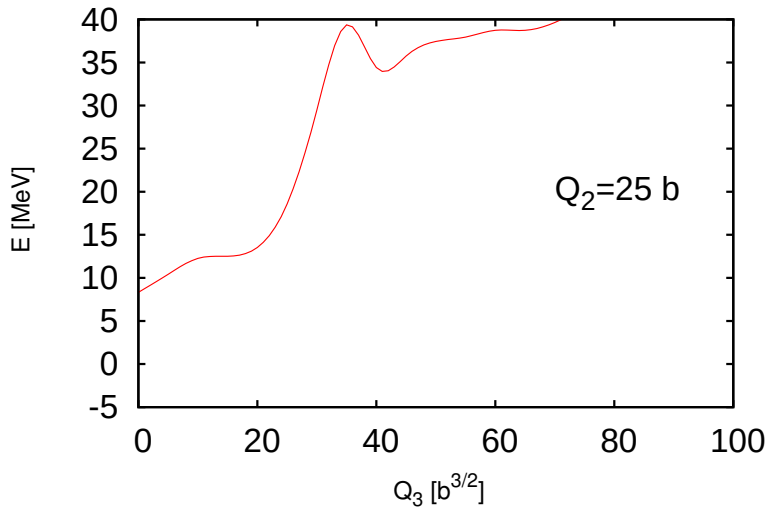

Ścieżka emisji klastru: $^{234}_{92}$U

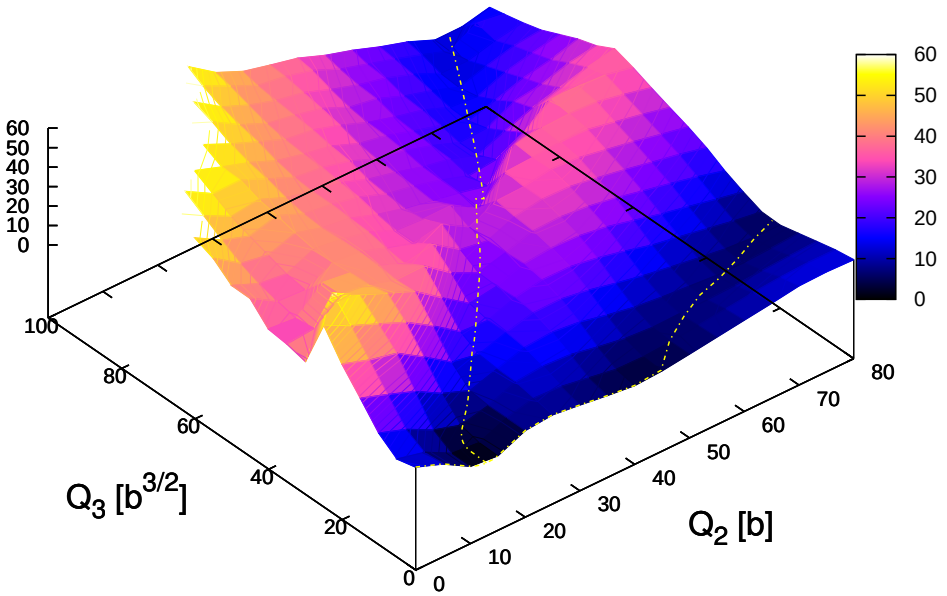

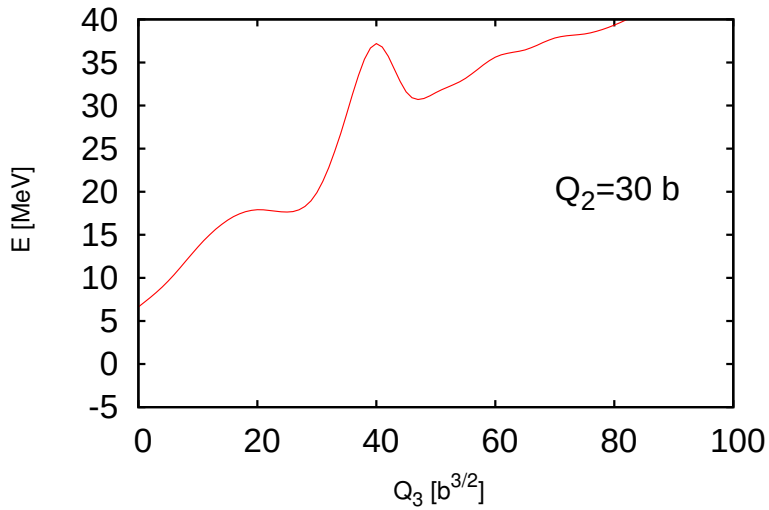

Ścieżka emisji klastru: $^{234}_{92}$U

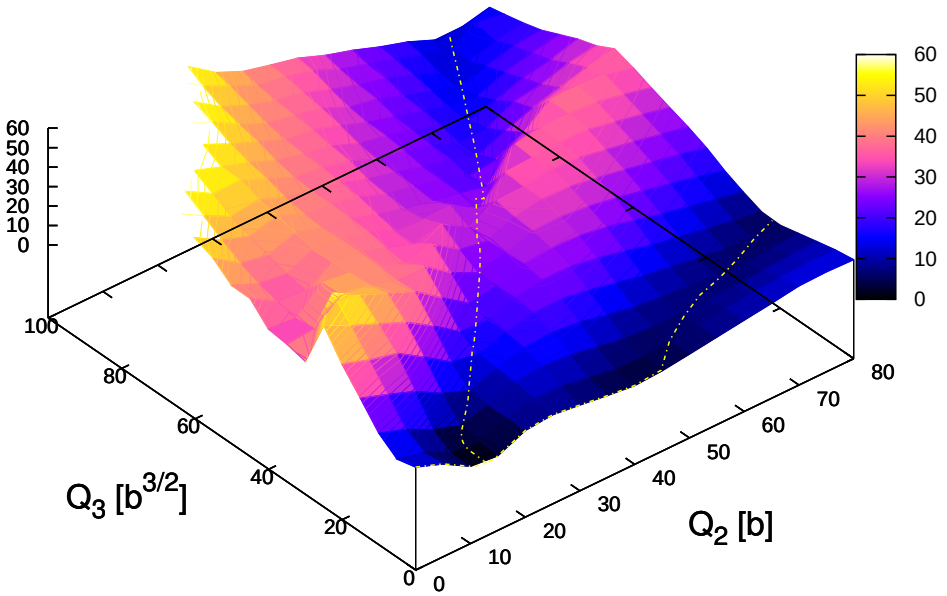

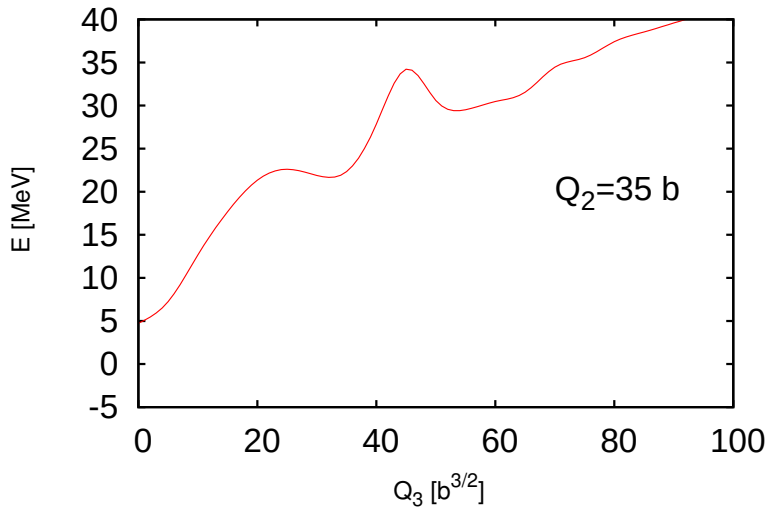

Ścieżka emisji klastru: $^{234}_{92}$U

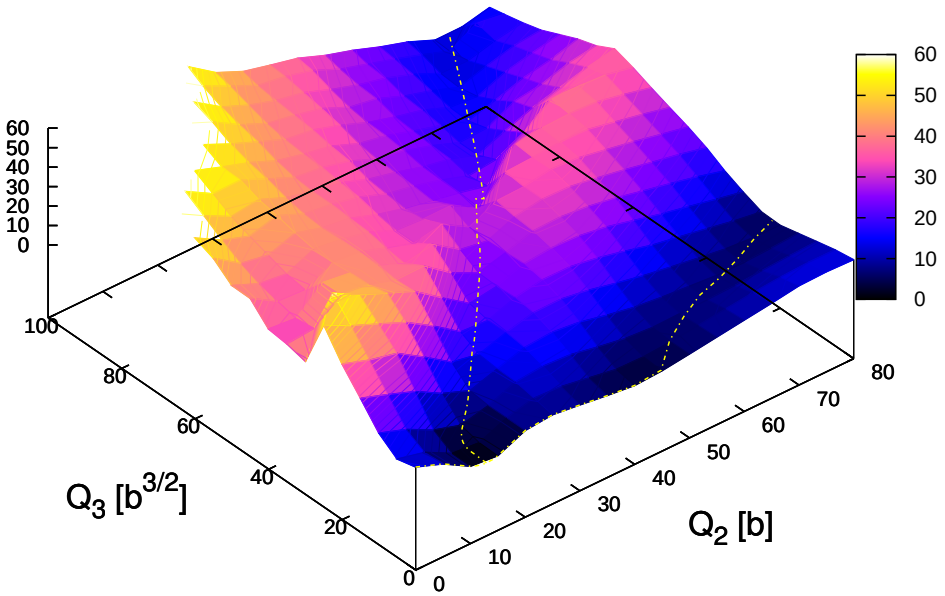

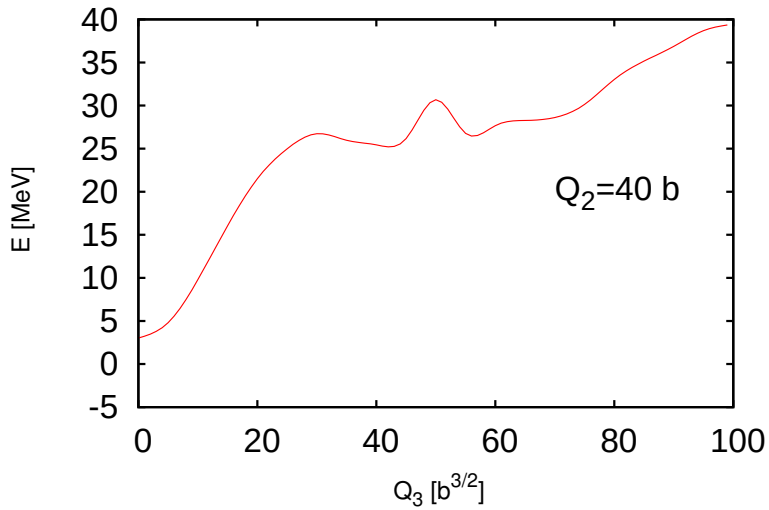

Ścieżka emisji klastru: $^{234}_{92}$U

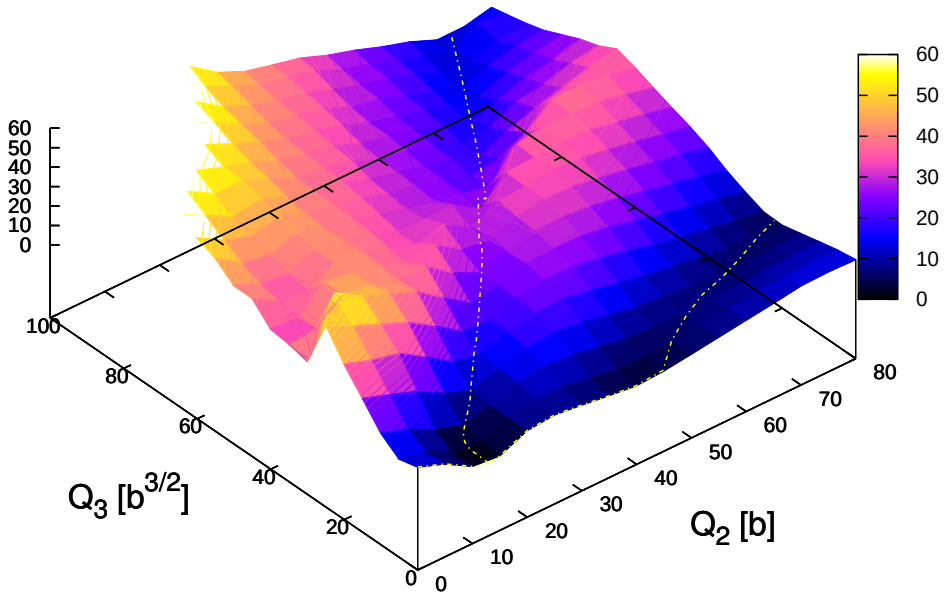

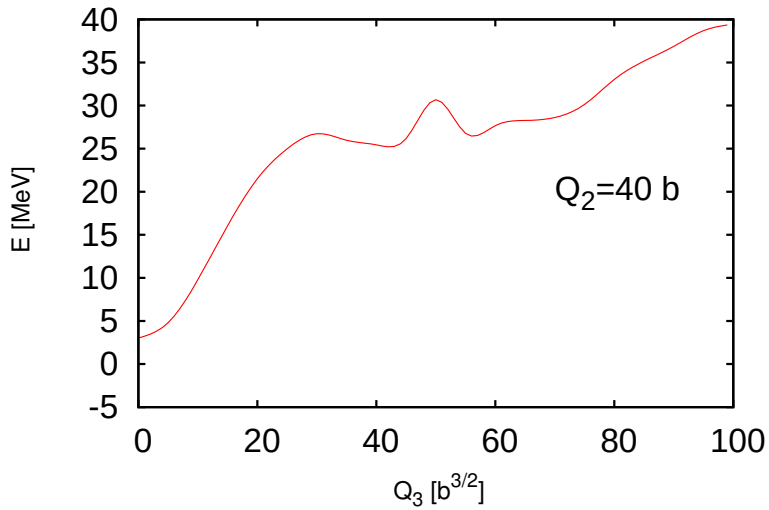

Nie można znaleźć ścieżki rozpadu prowadzącej do powstania klastru jako minimum energii dla danego Q_2!

Ścieżka emisji klastru: $^{234}_{92}$U

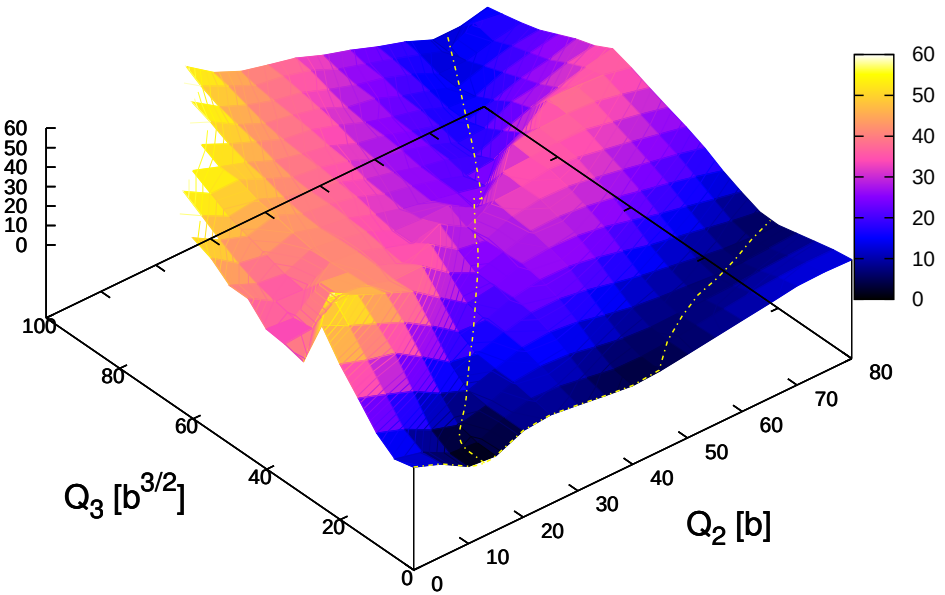

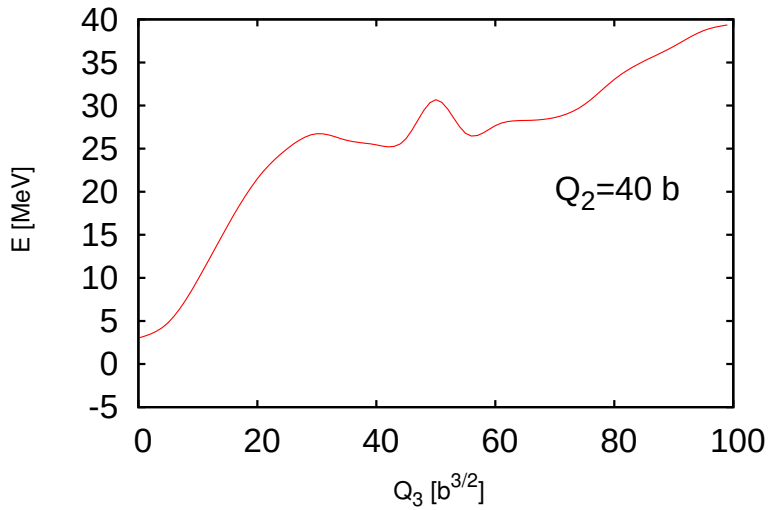

Nie można znaleźć ścieżki rozpadu prowadzącej do powstania klastru jako minimum energii dla danego Q_2!

ROZWIĄZANIE: współrzędna wiodąca – Q_3 !!!

Ścieżka emisji klastru: $^{234}_{92}$U

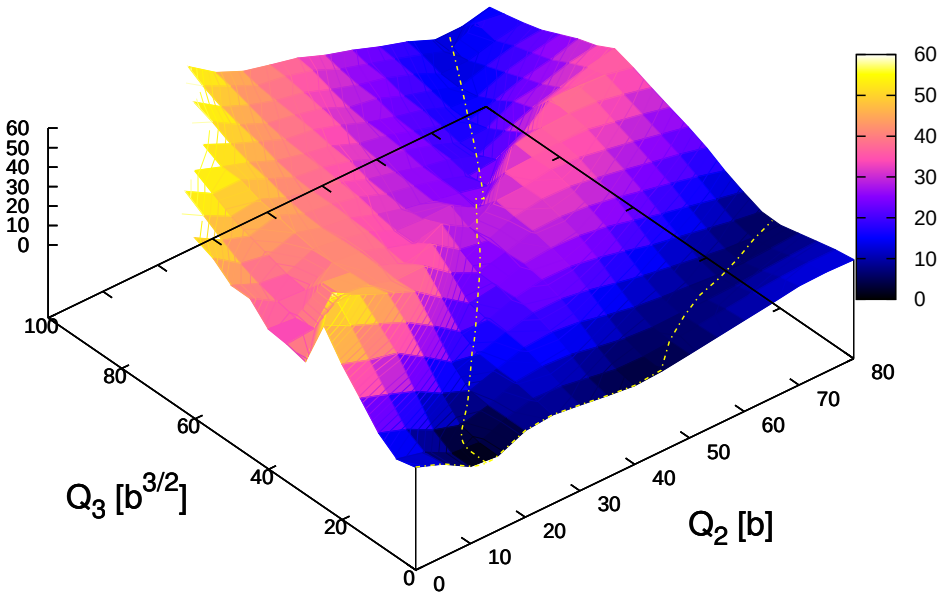

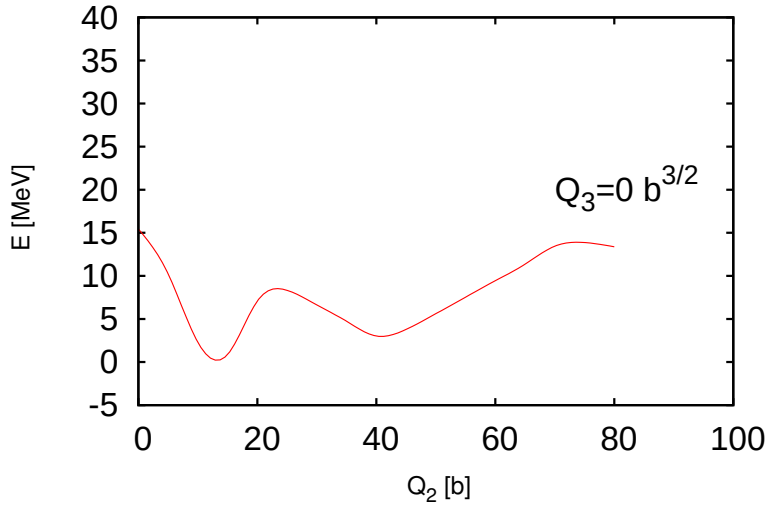

Nie można znaleźć ścieżki rozpadu prowadzącej do powstania klastru jako minimum energii dla danego Q_2!

ROZWIĄZANIE: współrzędna wiodąca – Q_3 !!!

Ścieżka emisji klastru: $^{234}_{92}$U

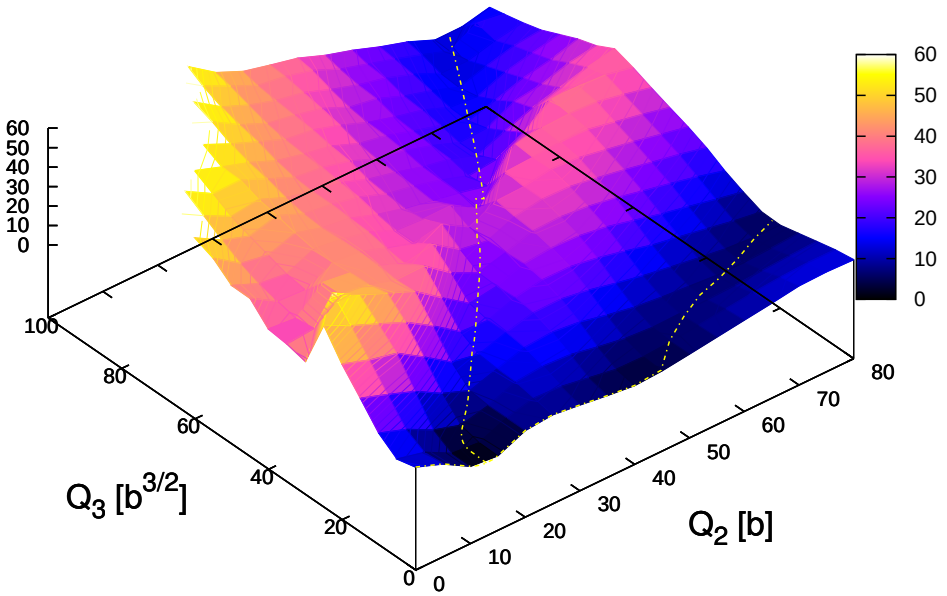

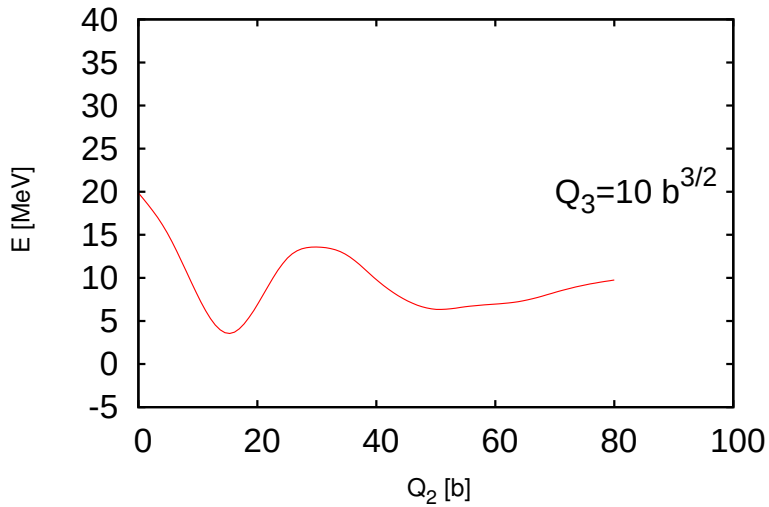

Ścieżka emisji klastru: $^{234}_{92}$U

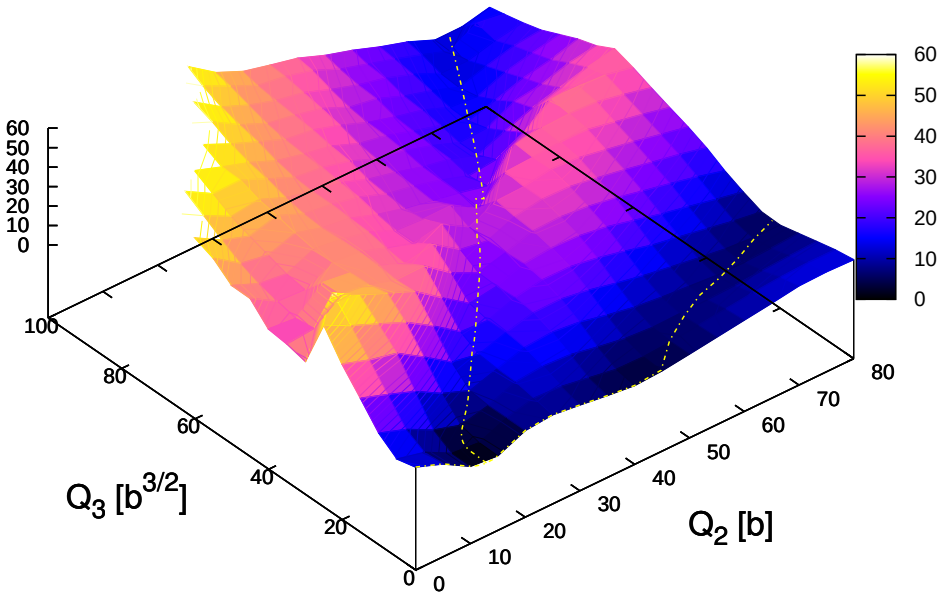

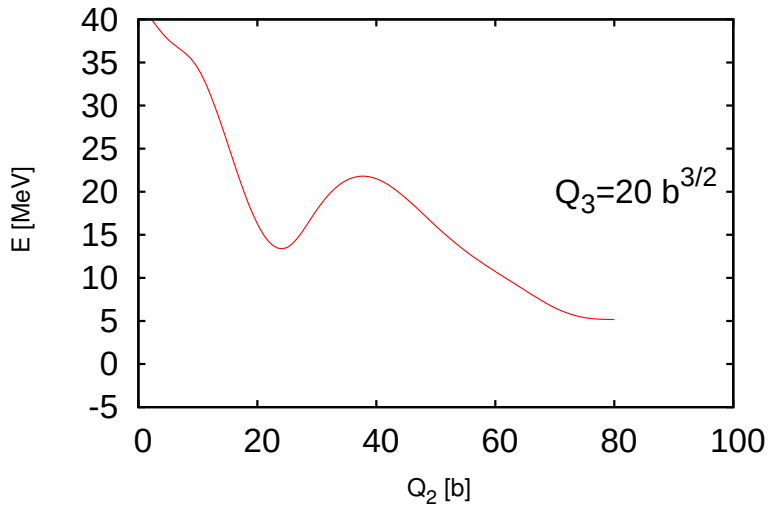

Ścieżka emisji klastru: $^{234}_{92}$U

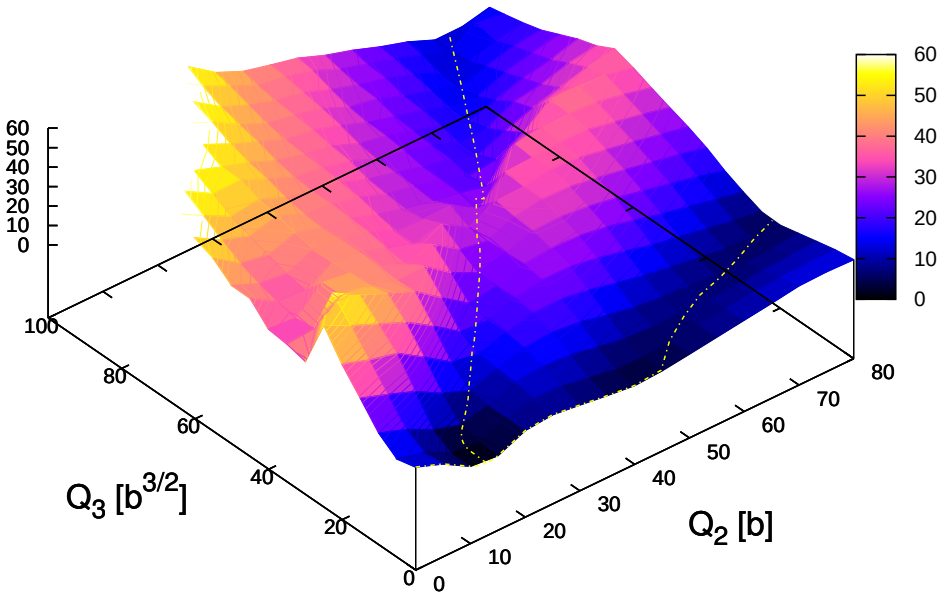

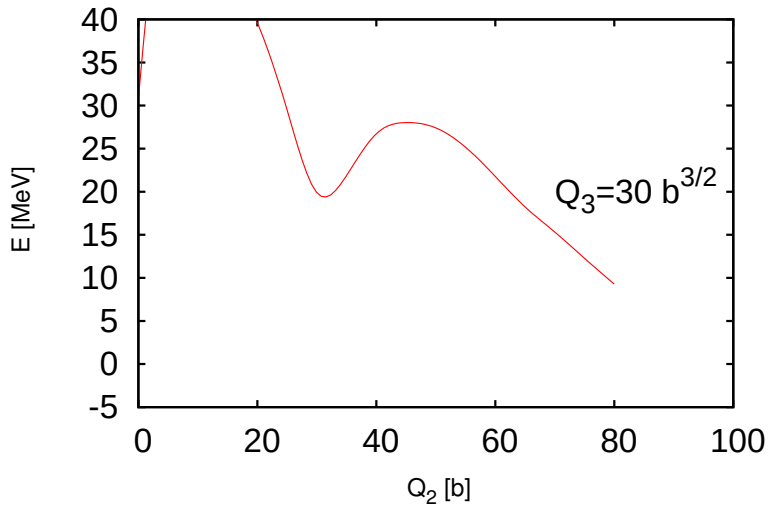

Ścieżka emisji klastru: $^{234}_{92}$U

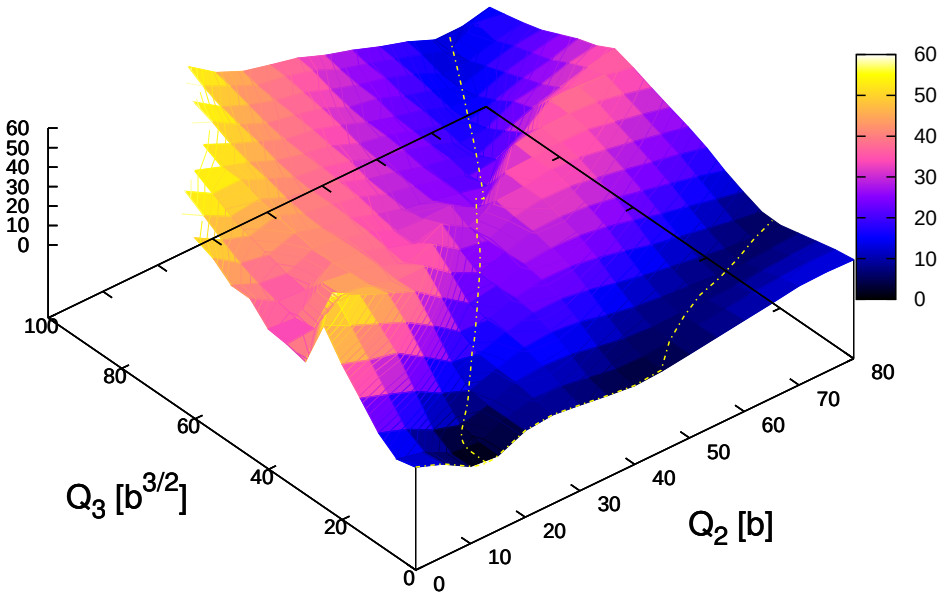

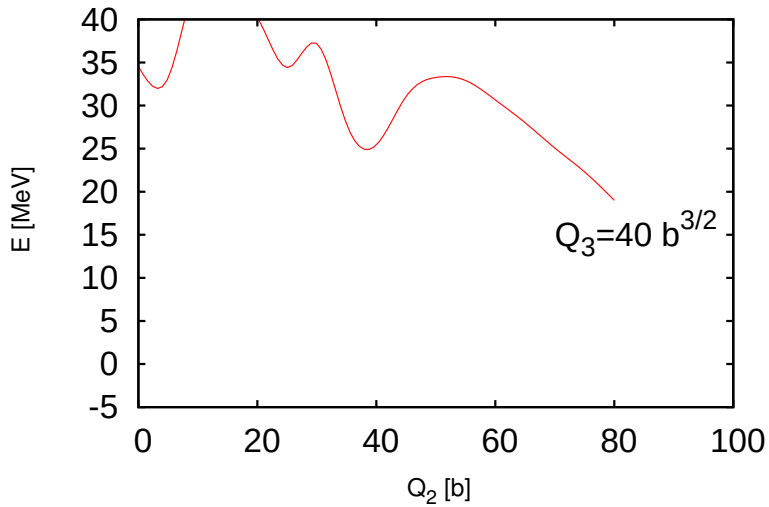

Ścieżka emisji klastru: ^{234}U

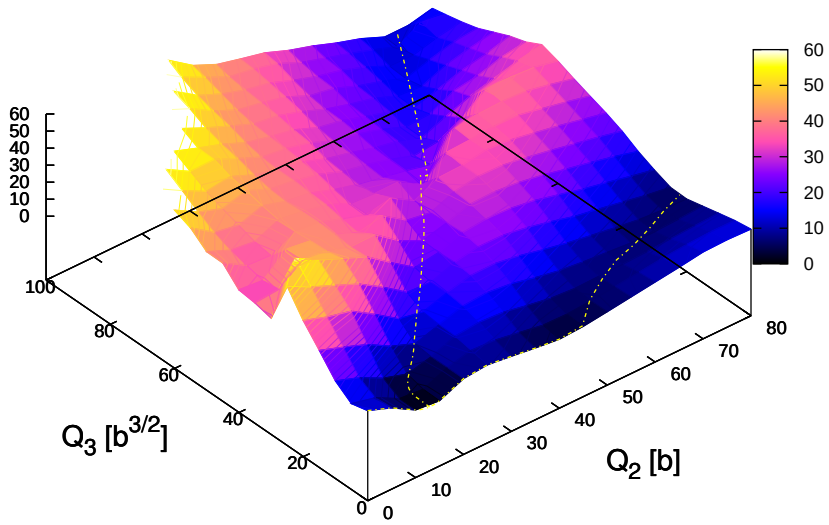

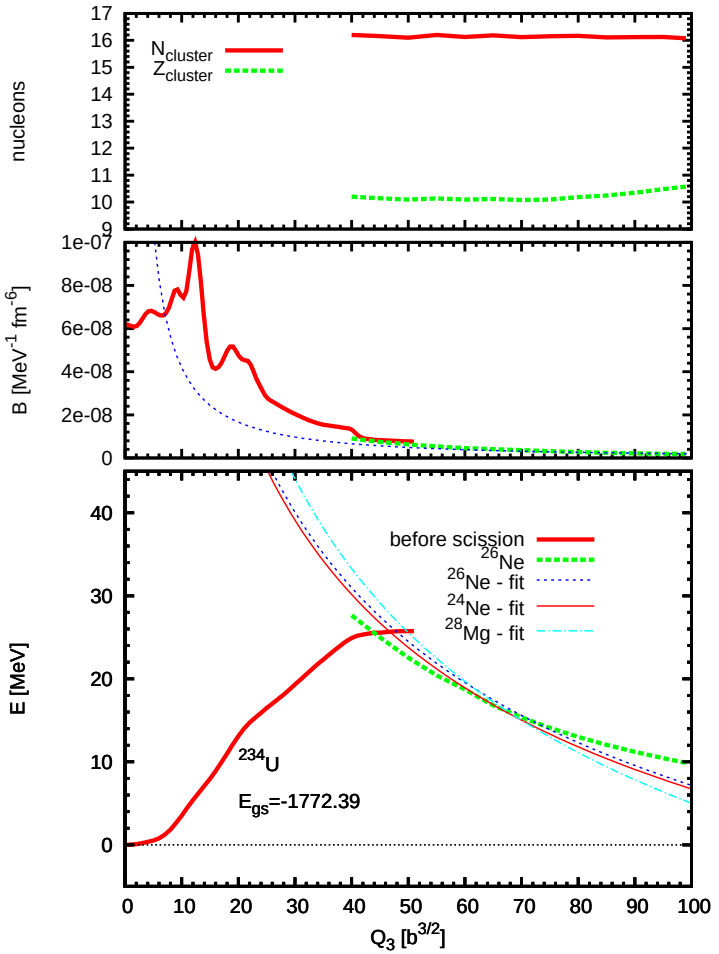

Ewolucja kształtu: ^{234}U

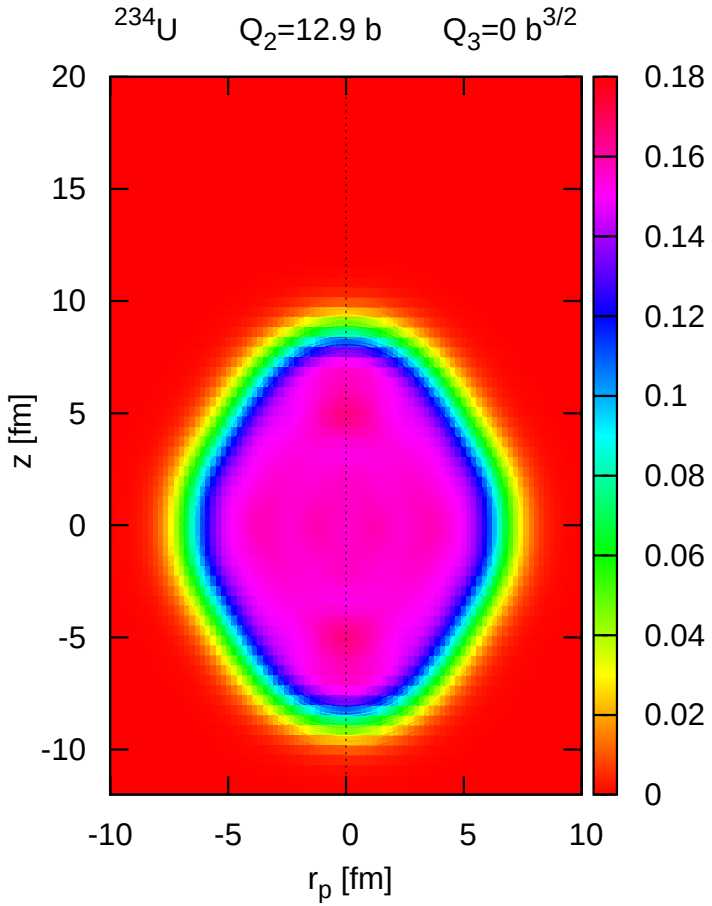

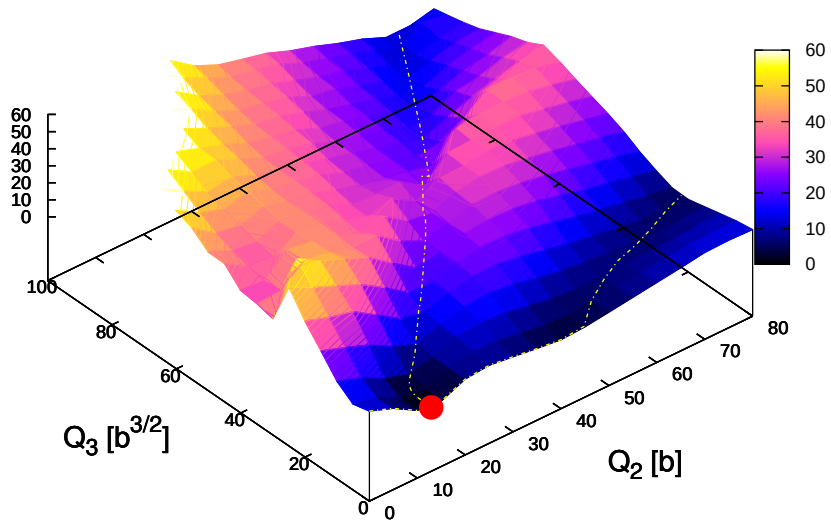

Ewolucja kształtu: ^{234}U

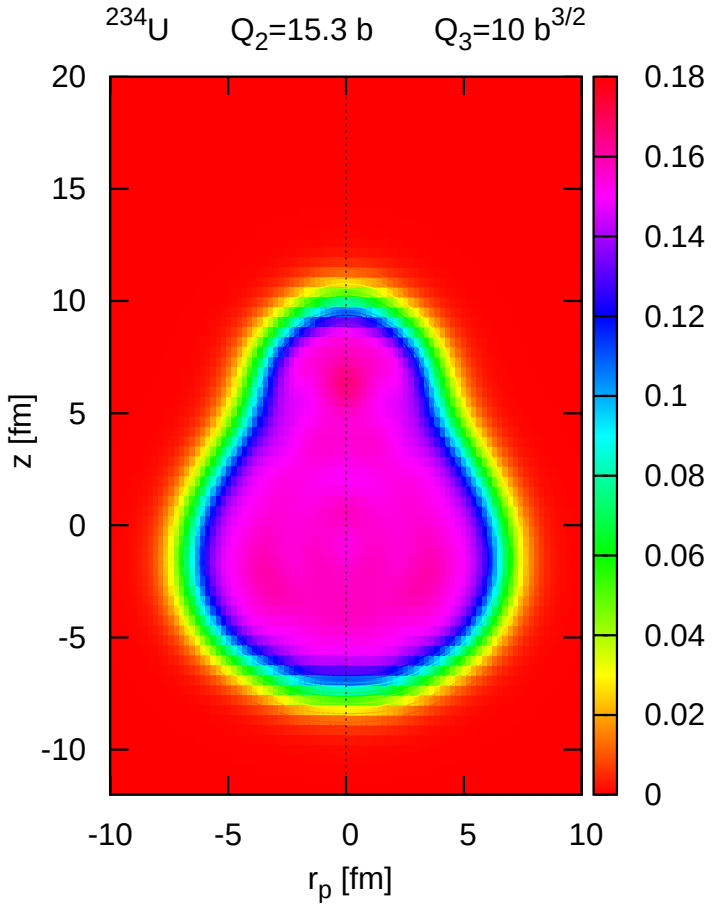

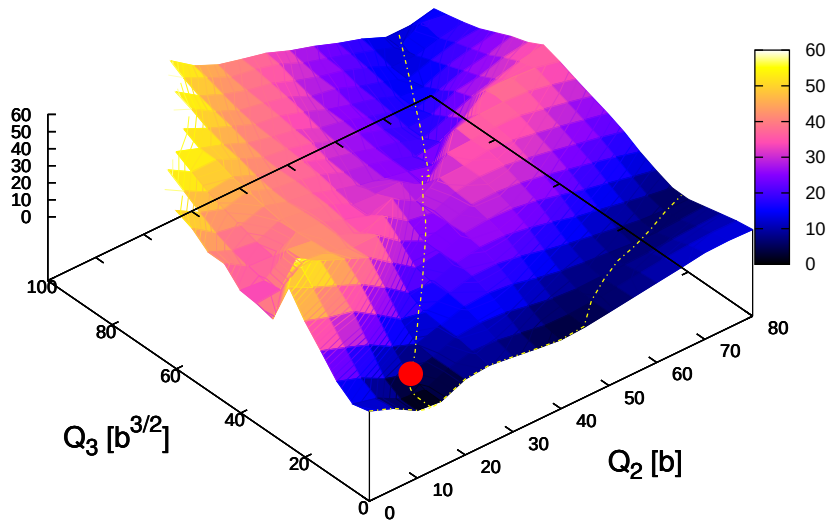

Ewolucja kształtu: ^{234}U

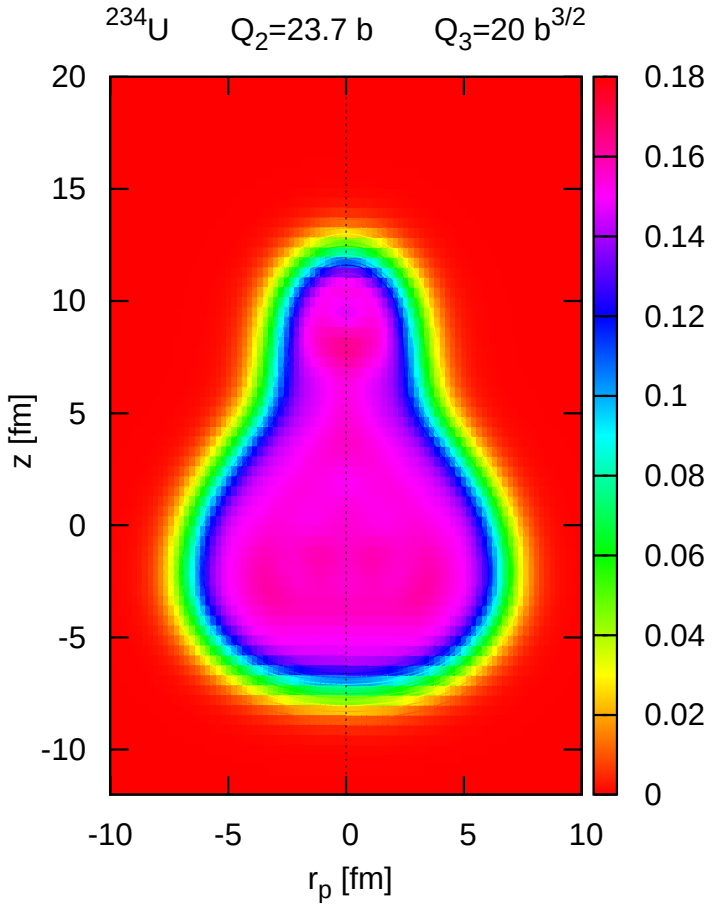

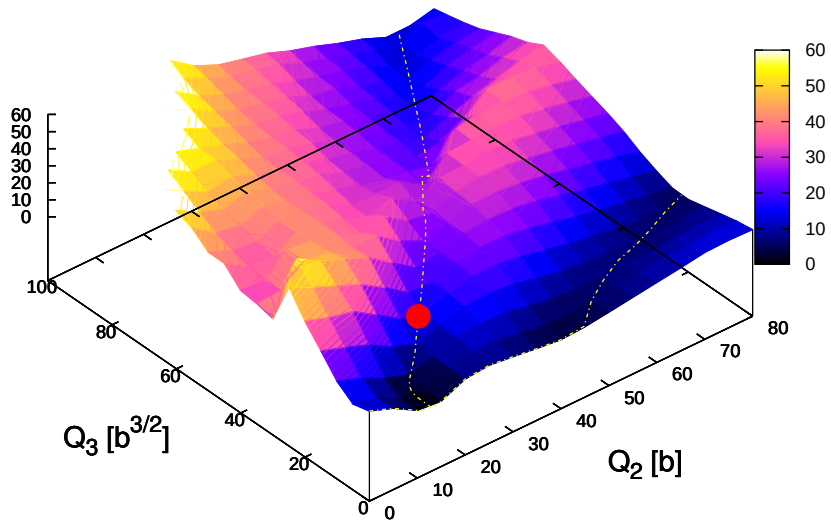

Ewolucja kształtu: ^{234}U

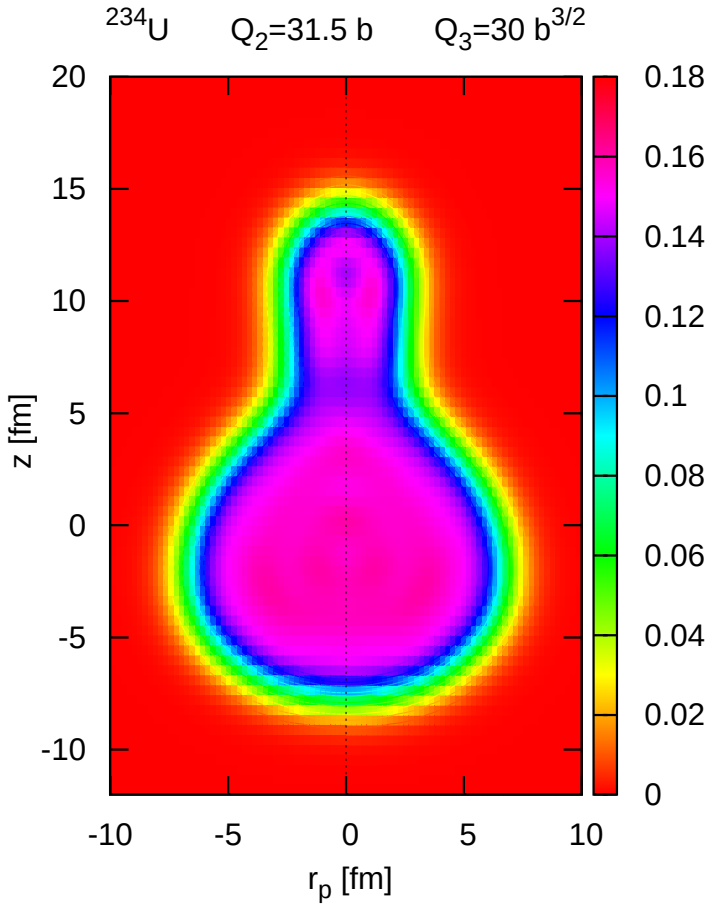

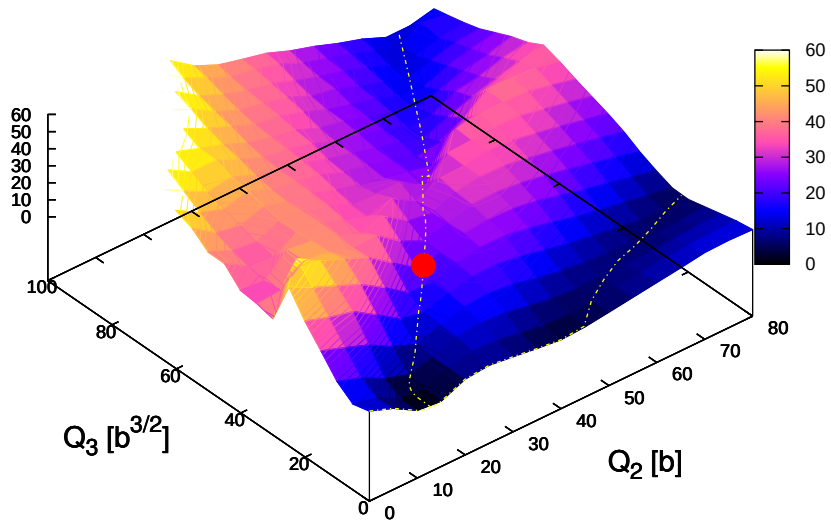

Ewolucja kształtu: ^{234}U

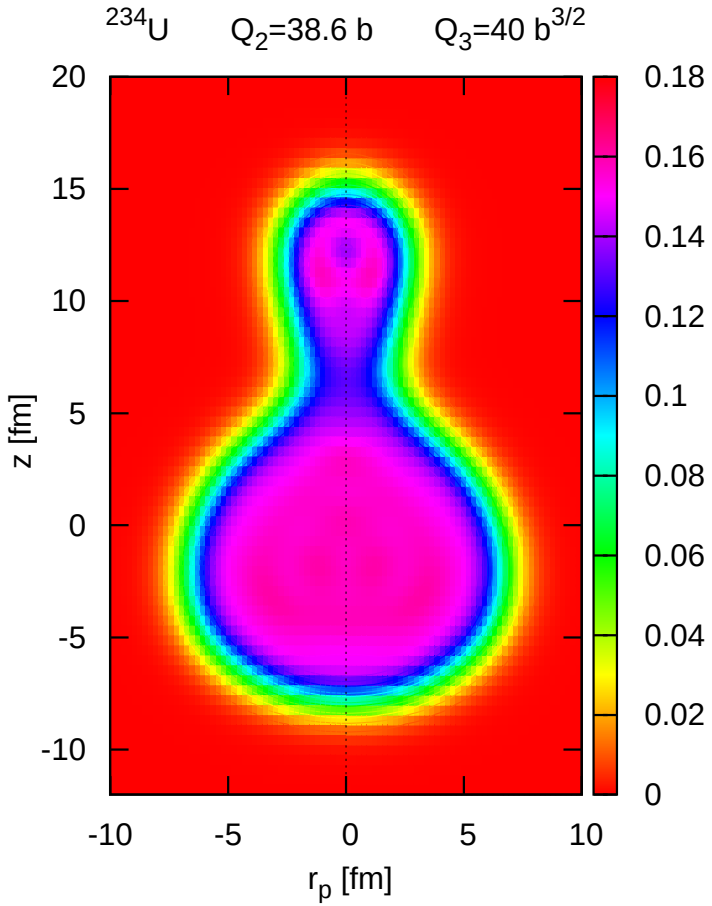

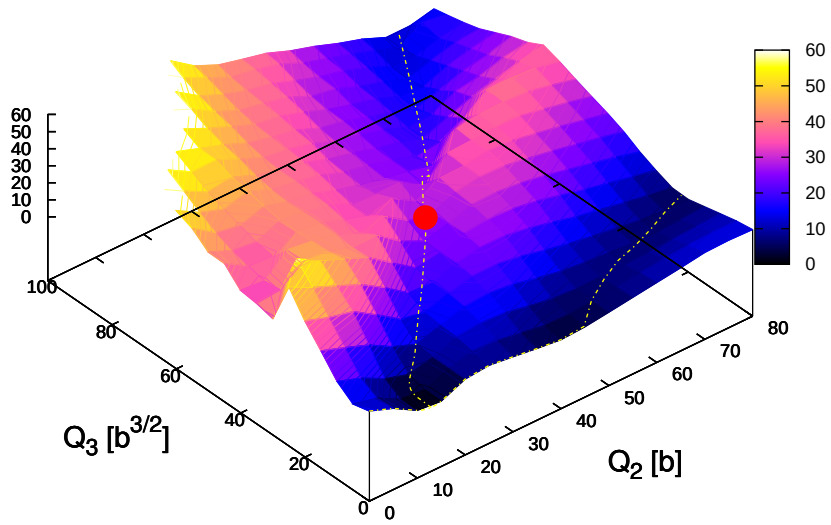

Ewolucja kształtu: ^{234}U

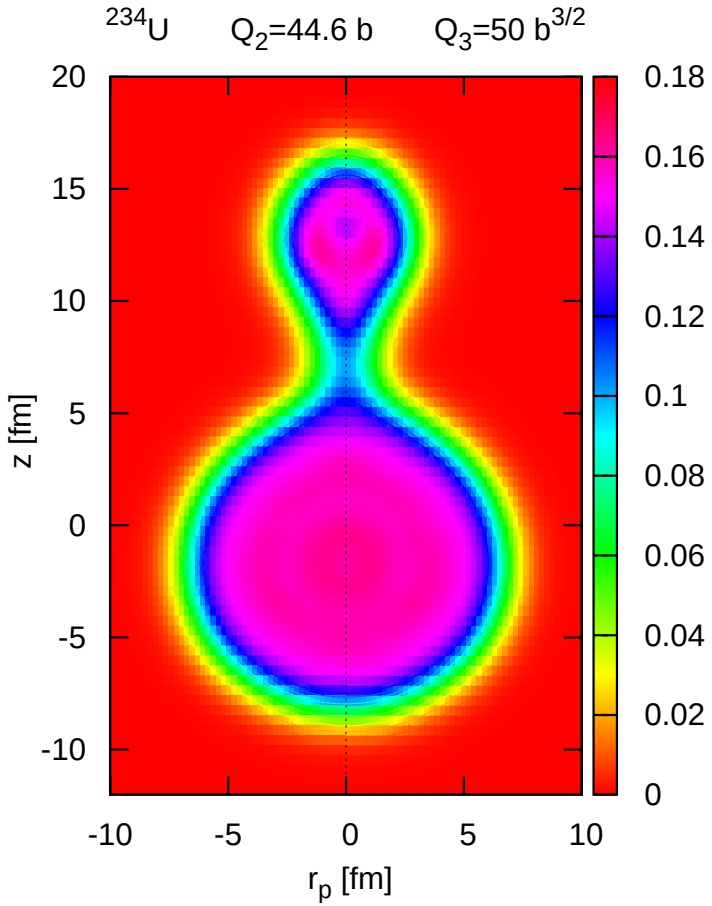

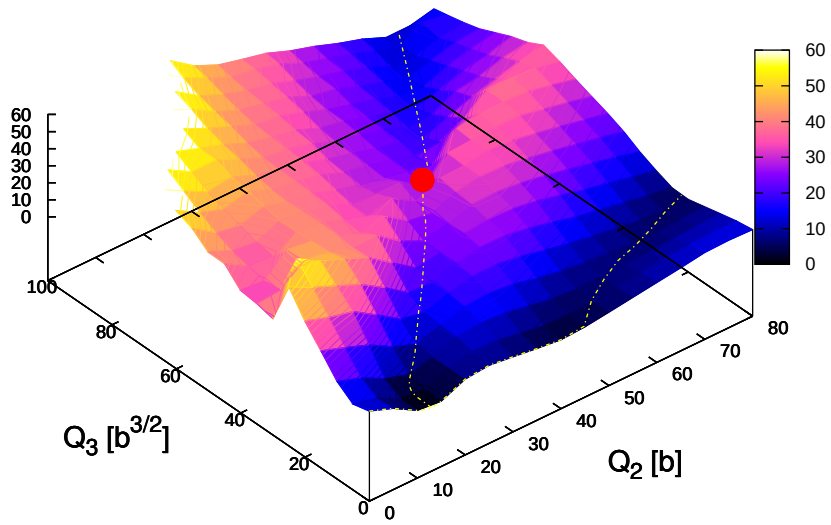

Ewolucja kształtu: ^{234}U

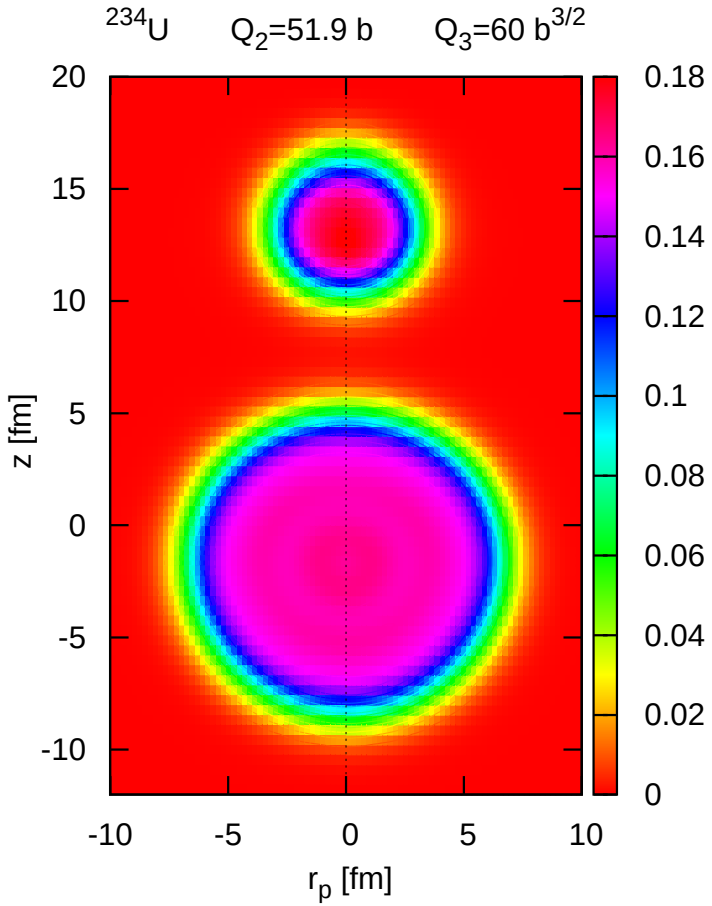

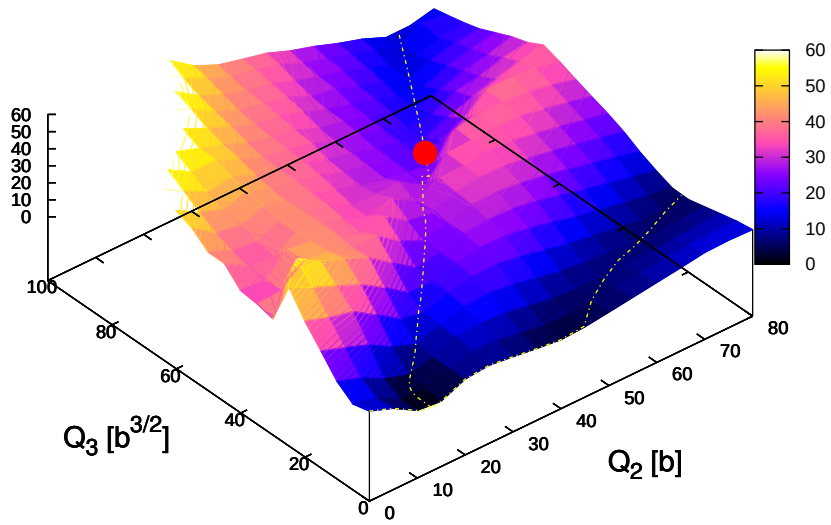

Ewolucja kształtu: ^{234}U

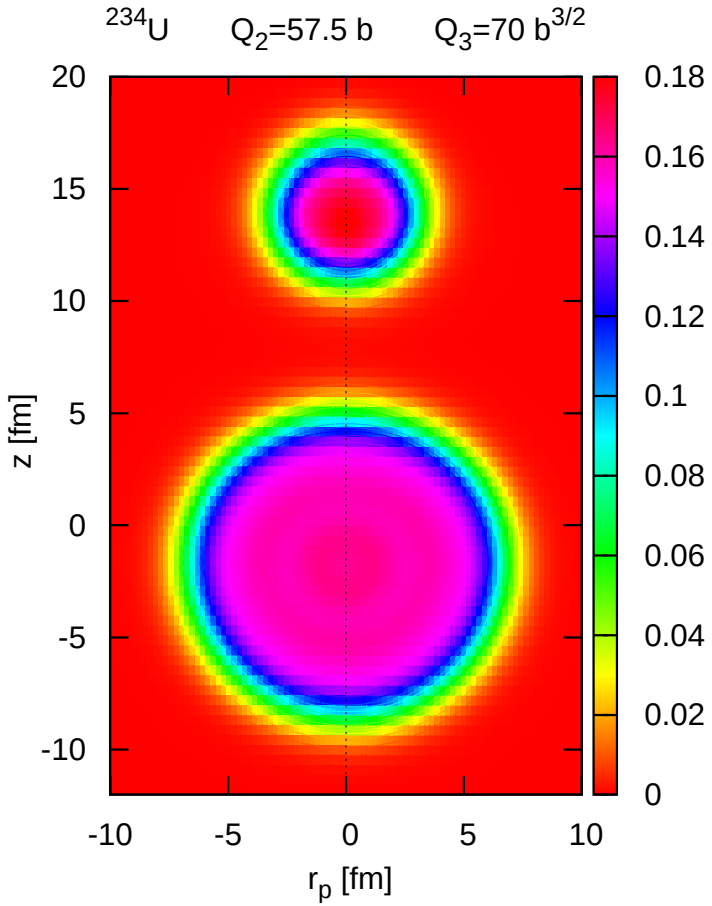

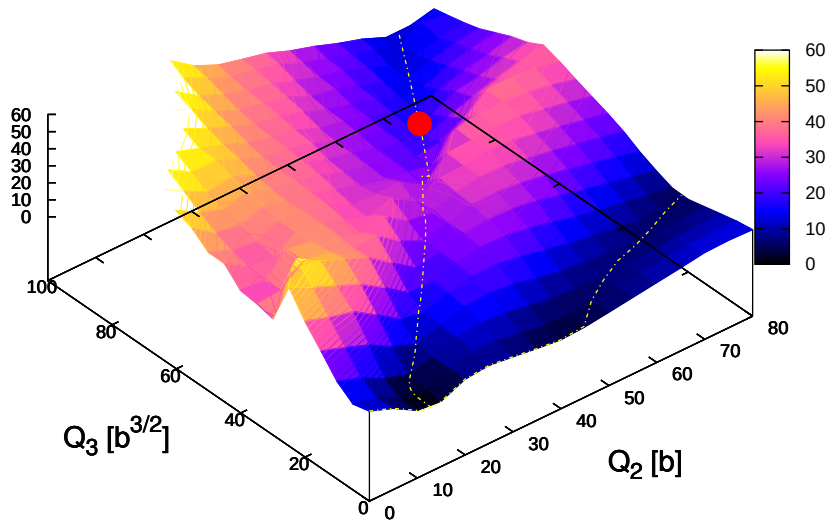

Ewolucja kształtu: ^{234}U

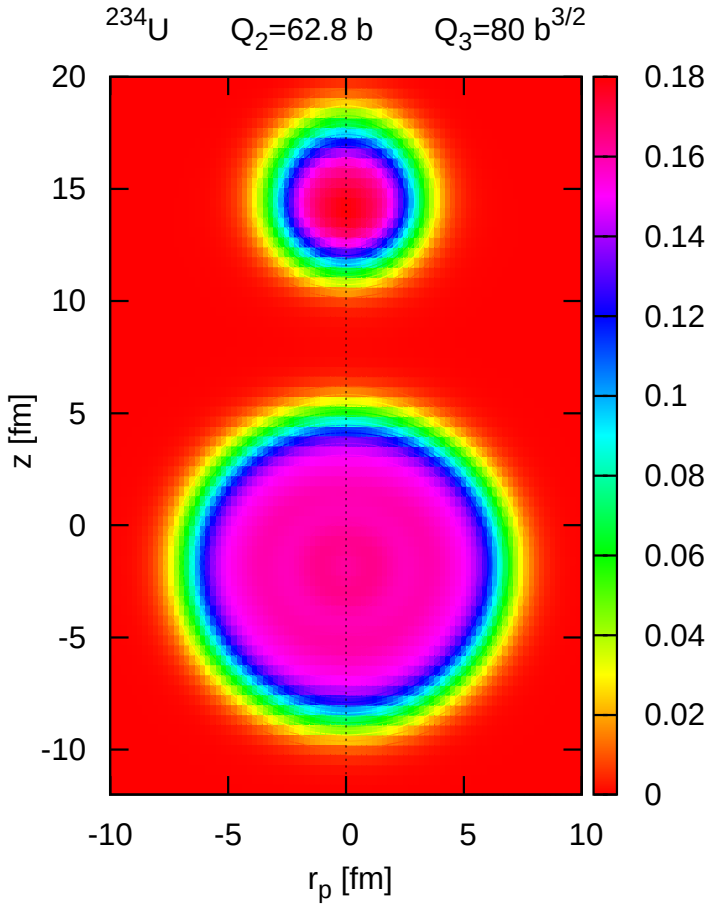

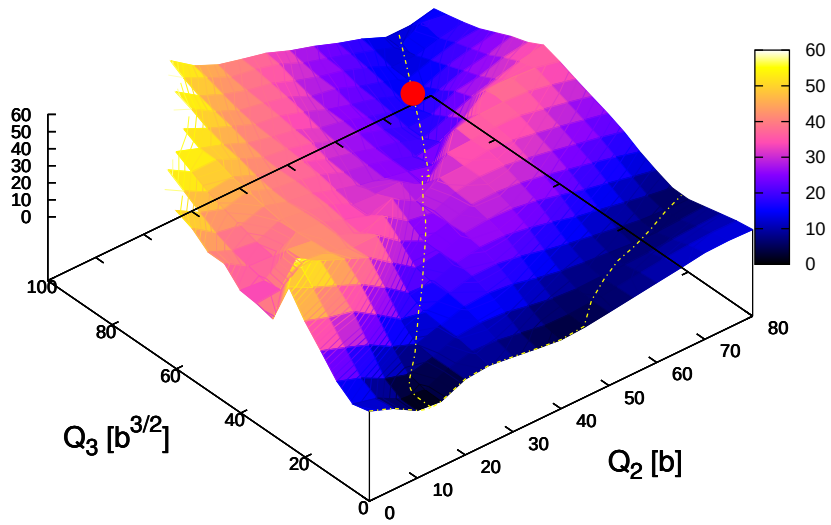

Ewolucja kształtu: ^{234}U

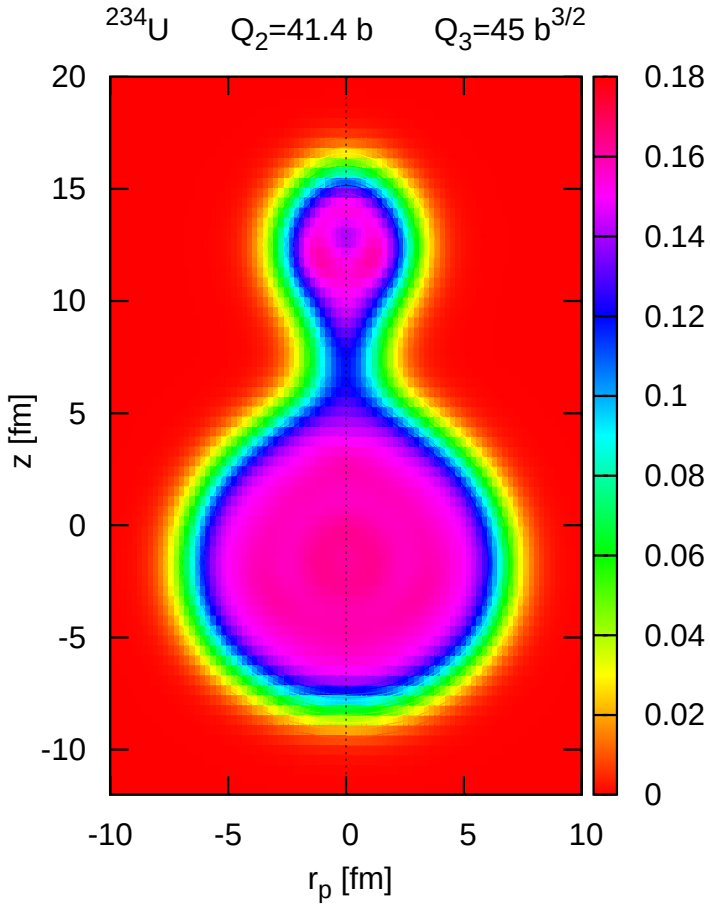

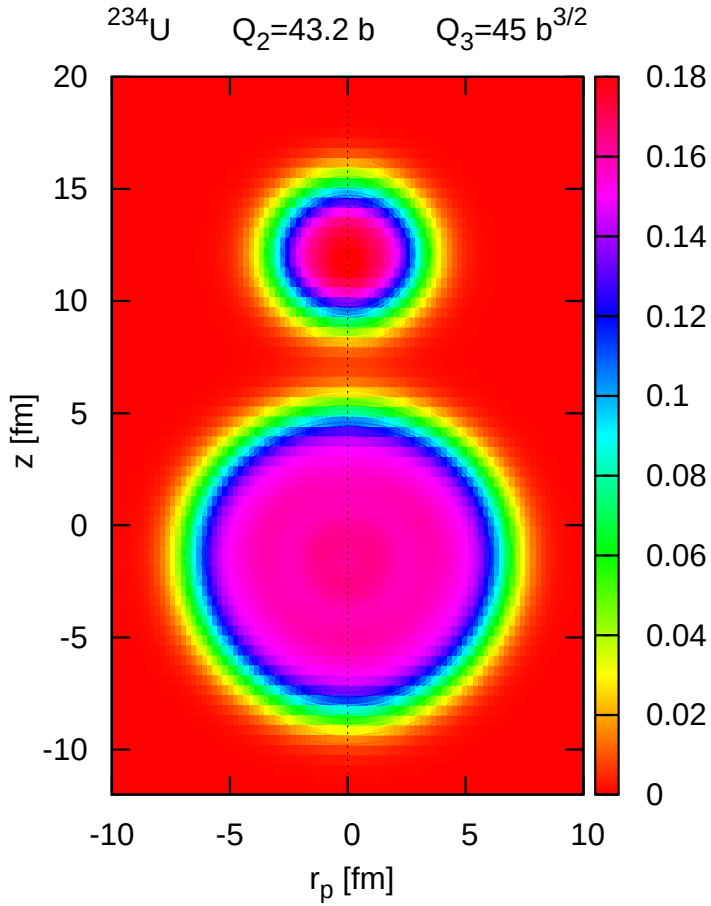

Ścieżka emisji klastru: ^{226}Ra

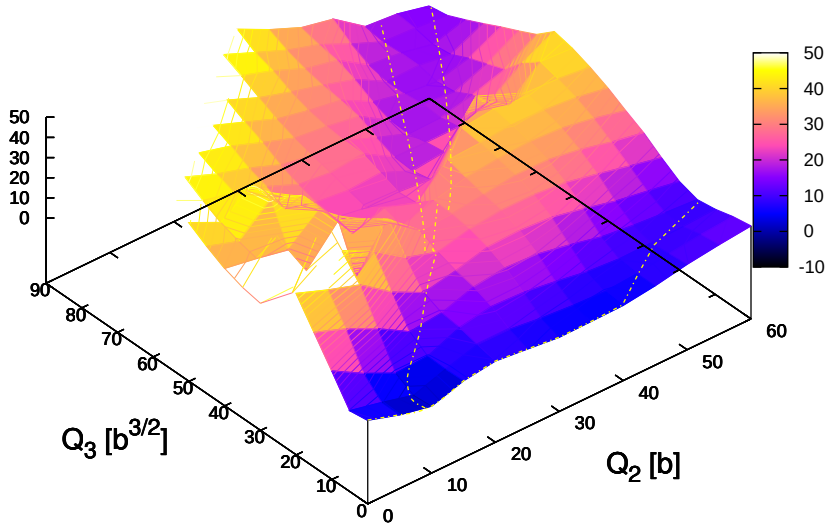

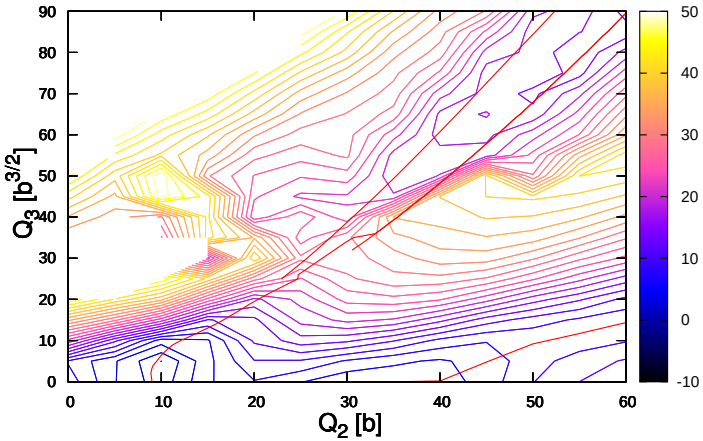

Ścieżka emisji klastru: ^{226}Ra

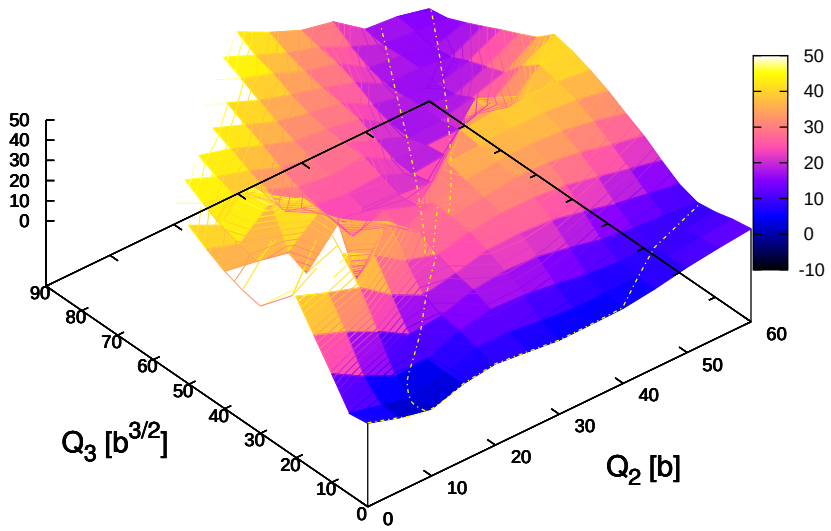

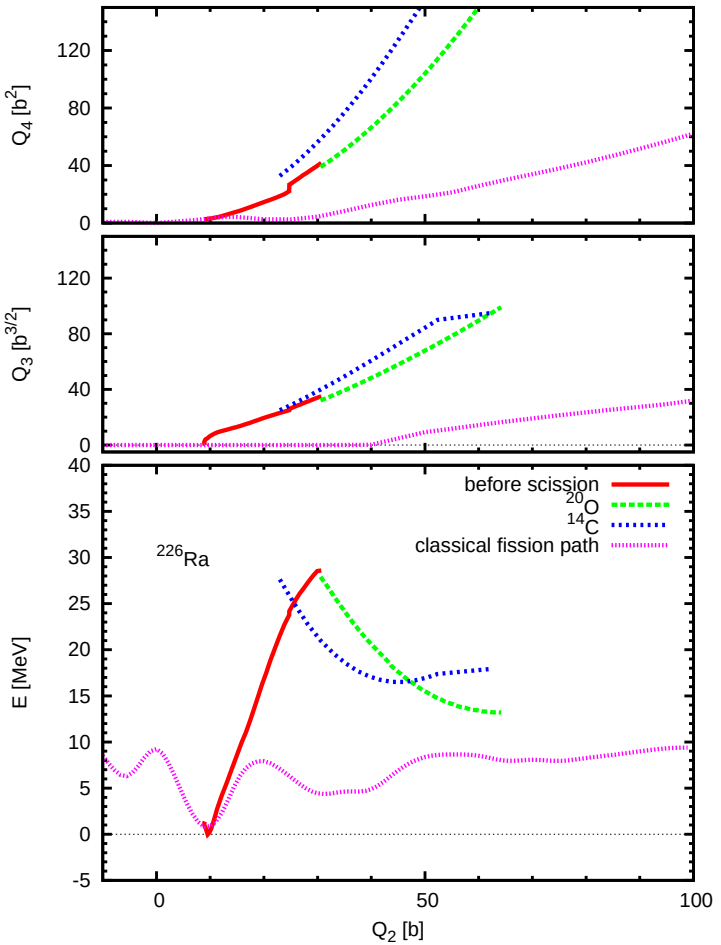

Ścieżka emisji klastru: ^{226}Ra

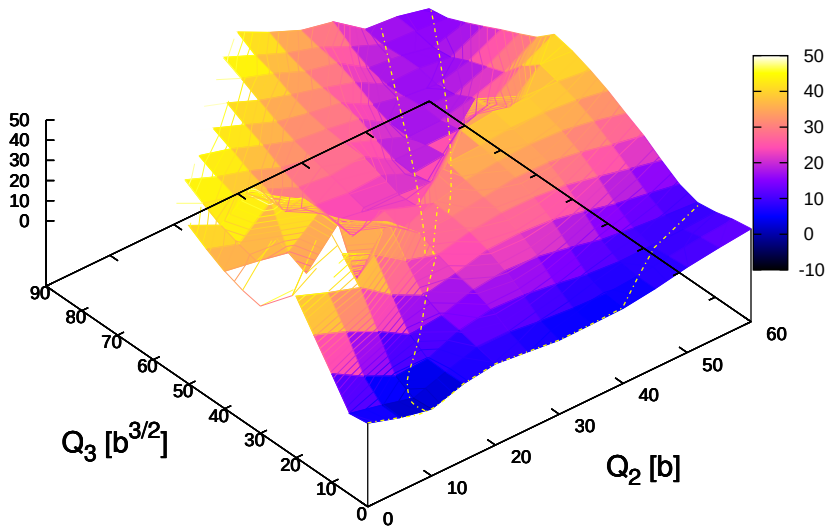

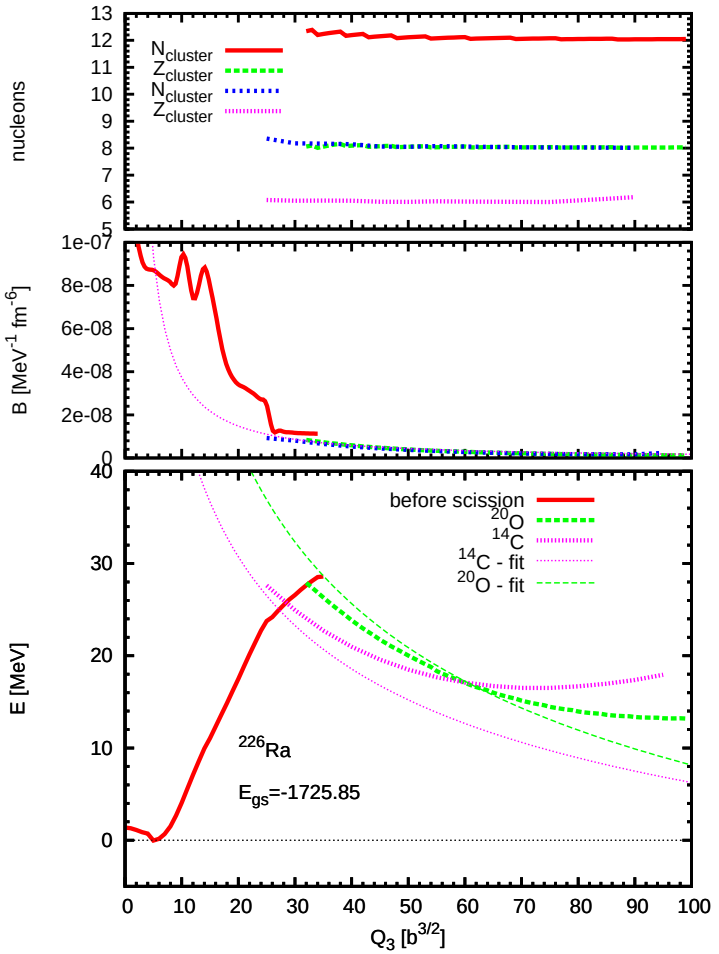

Ścieżka emisji klastru: ^{242}Cm

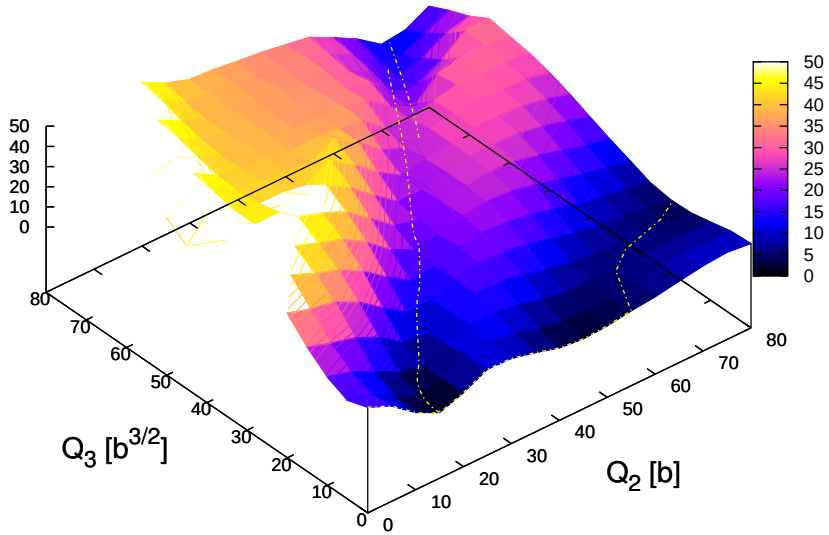

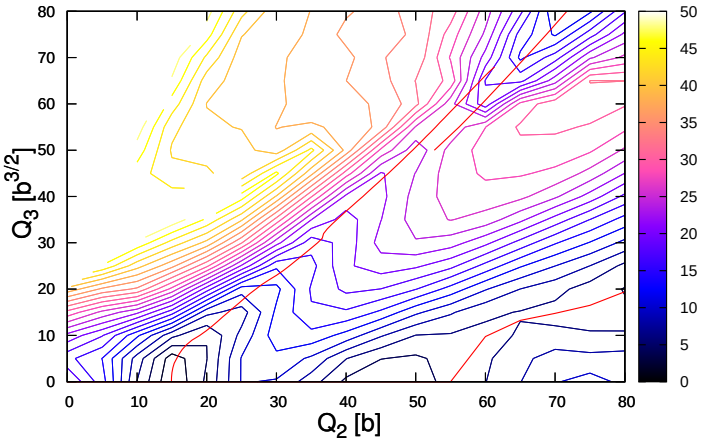

Ścieżka emisji klastru: ^{242}Cm

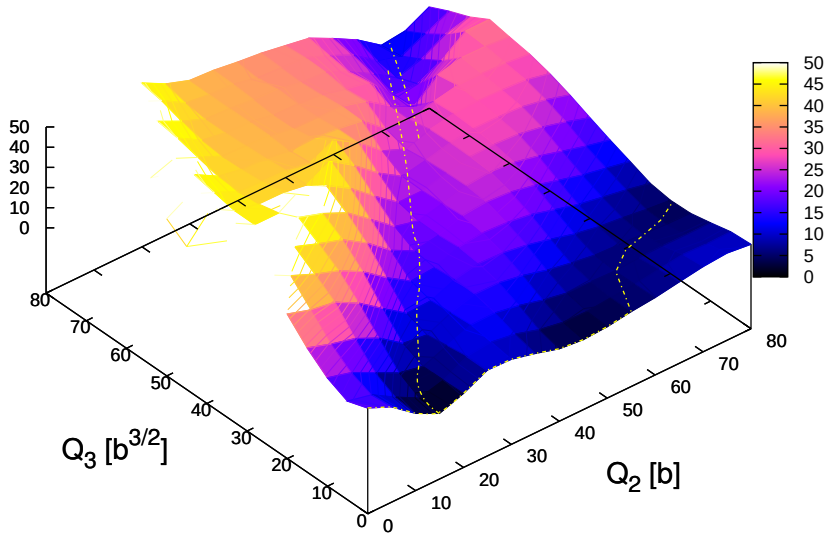

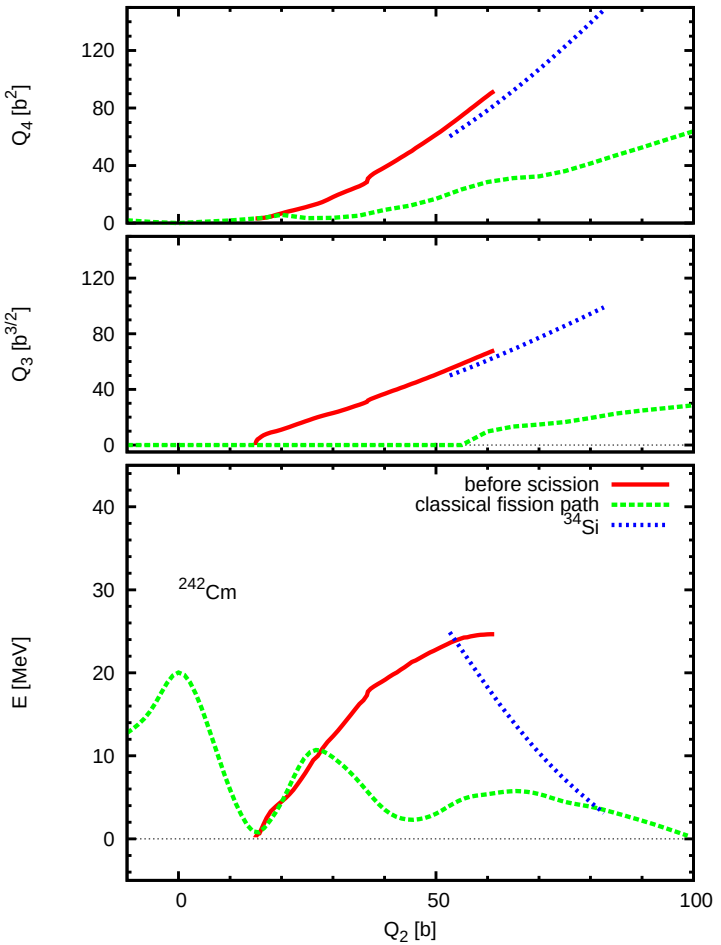

Ścieżka emisji klastru: ^{242}Cm

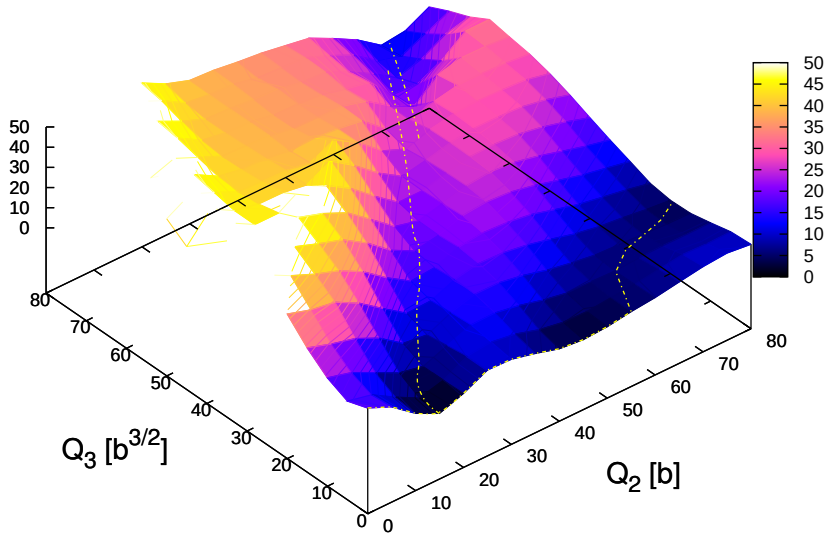

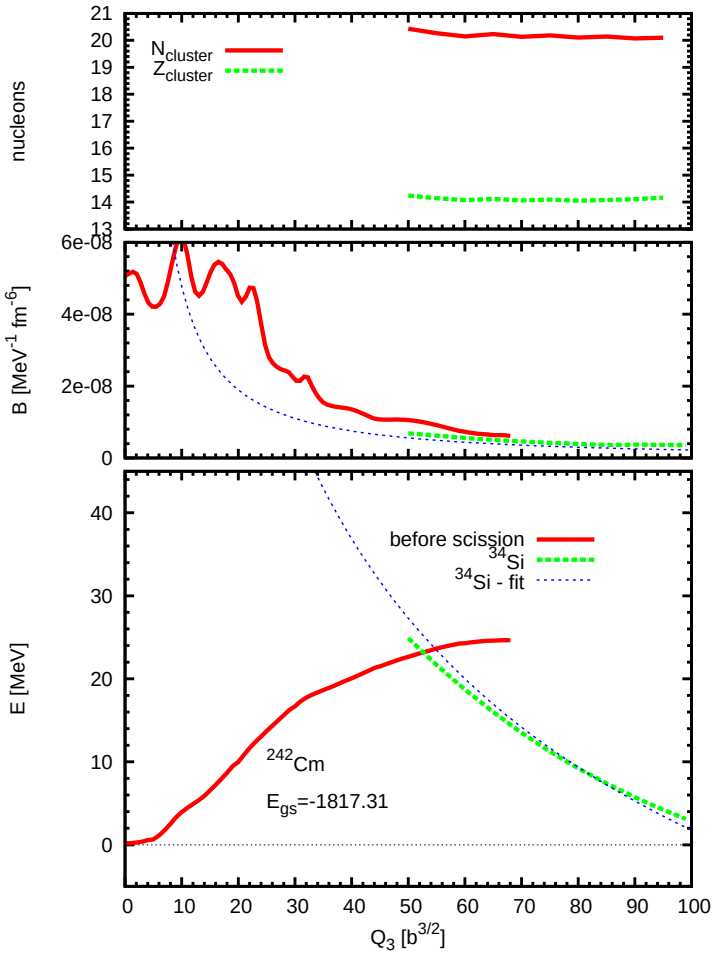

Dane doświadczalne

- G. Audi, et al. NPA 729 (2003) 3
- M. A. Hooshyar I. Reichstein F. B. Malik, *Nuclear Fission and Cluster Radioactivity - An Energy-Density Functional Approach* Springer-Verlag, Berlin Heidelberg, 2005
- R. Bonetti, A. Guglielmetti, in *Heavy Elements and Related New Phenomena Vol II, ed. W. Greiner and R.K. Gupta*, p.634, Word Scientific, 1999
- M. Balasubramaniam, et al. PRC 70, 017301 (2004)
- R. Bonetti, et al. NPA 686,64 (2001)

Czasy życia: Ra and Th

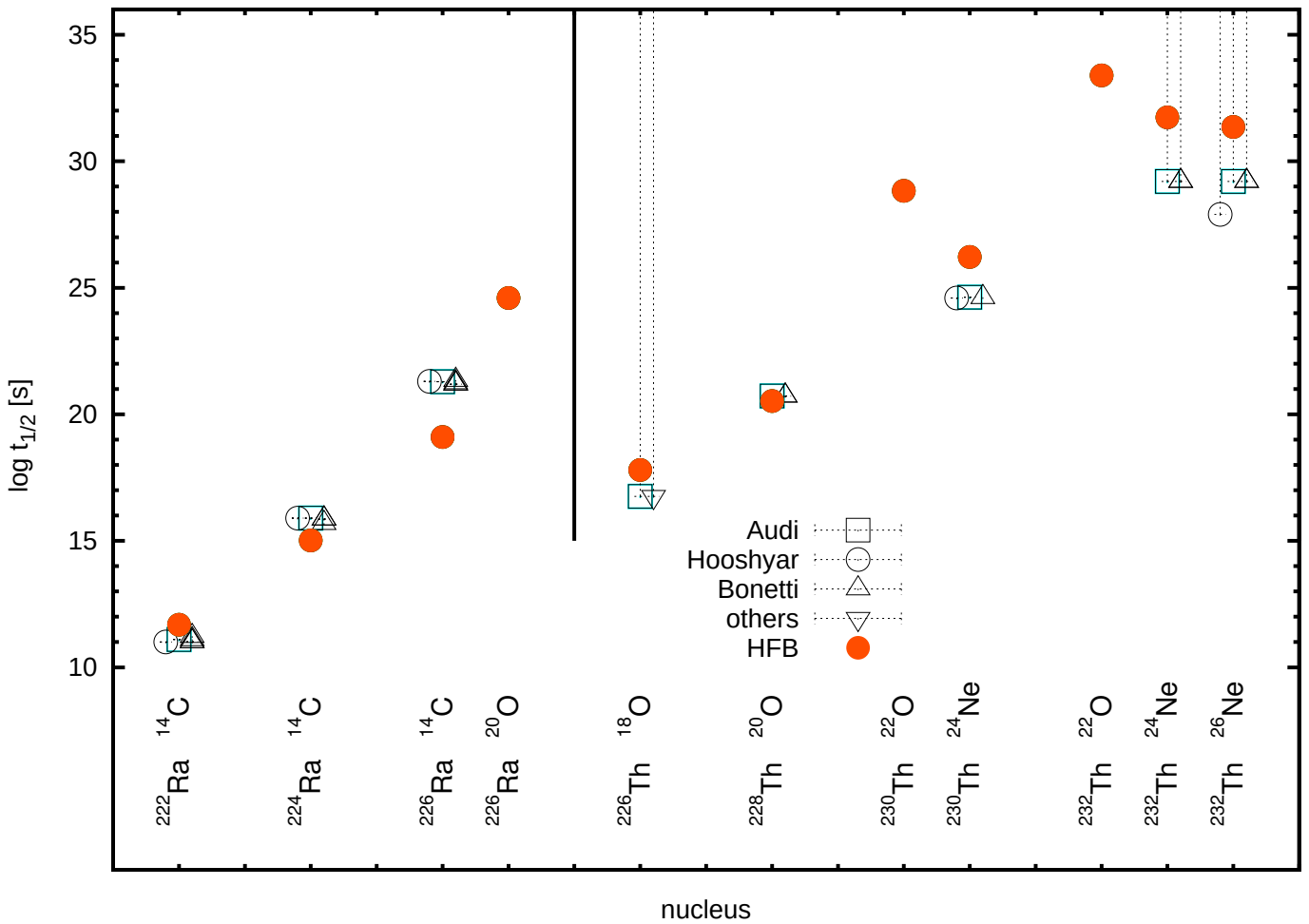

Czasy życia: U

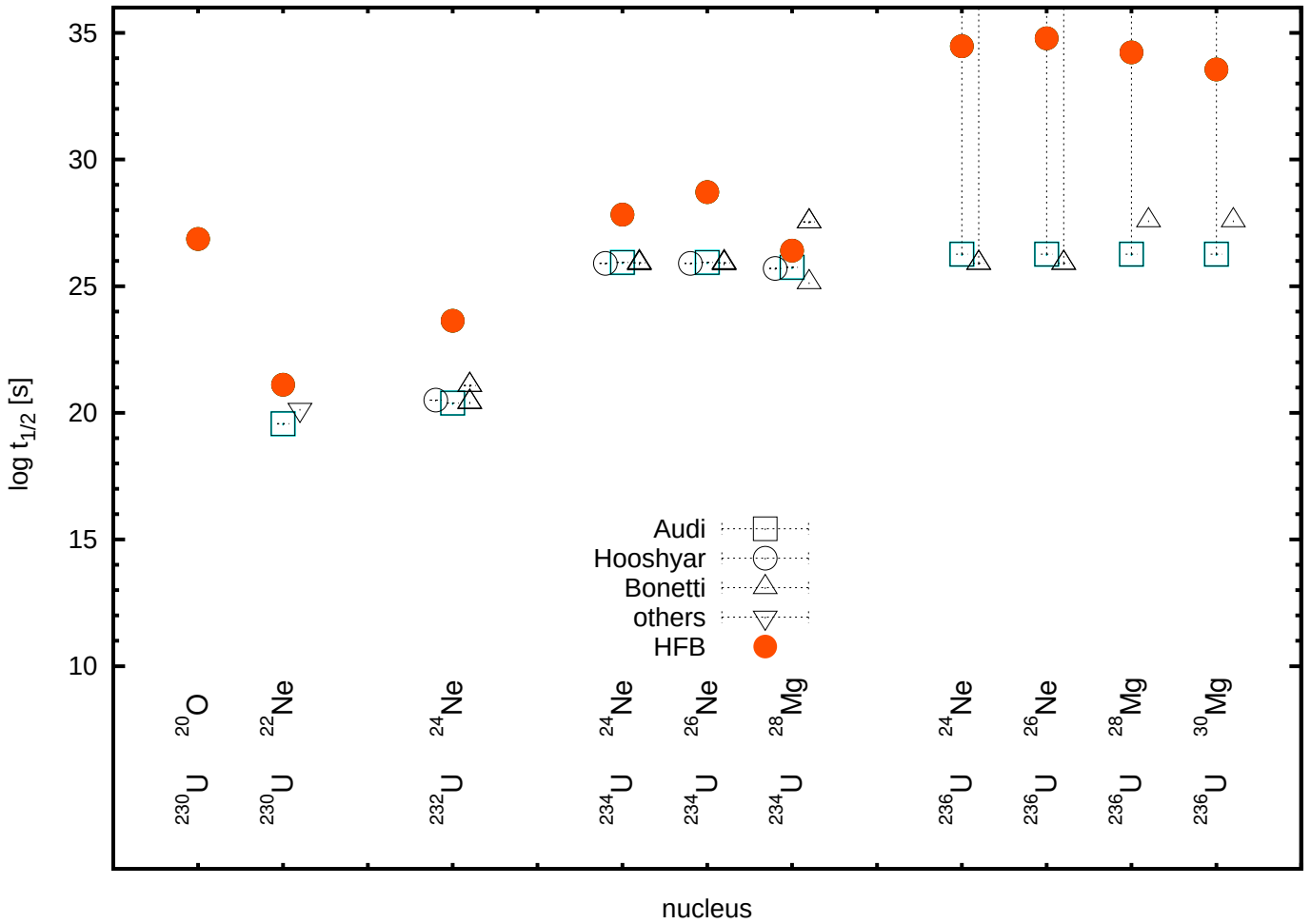

Czasy życia: Pu and Cm

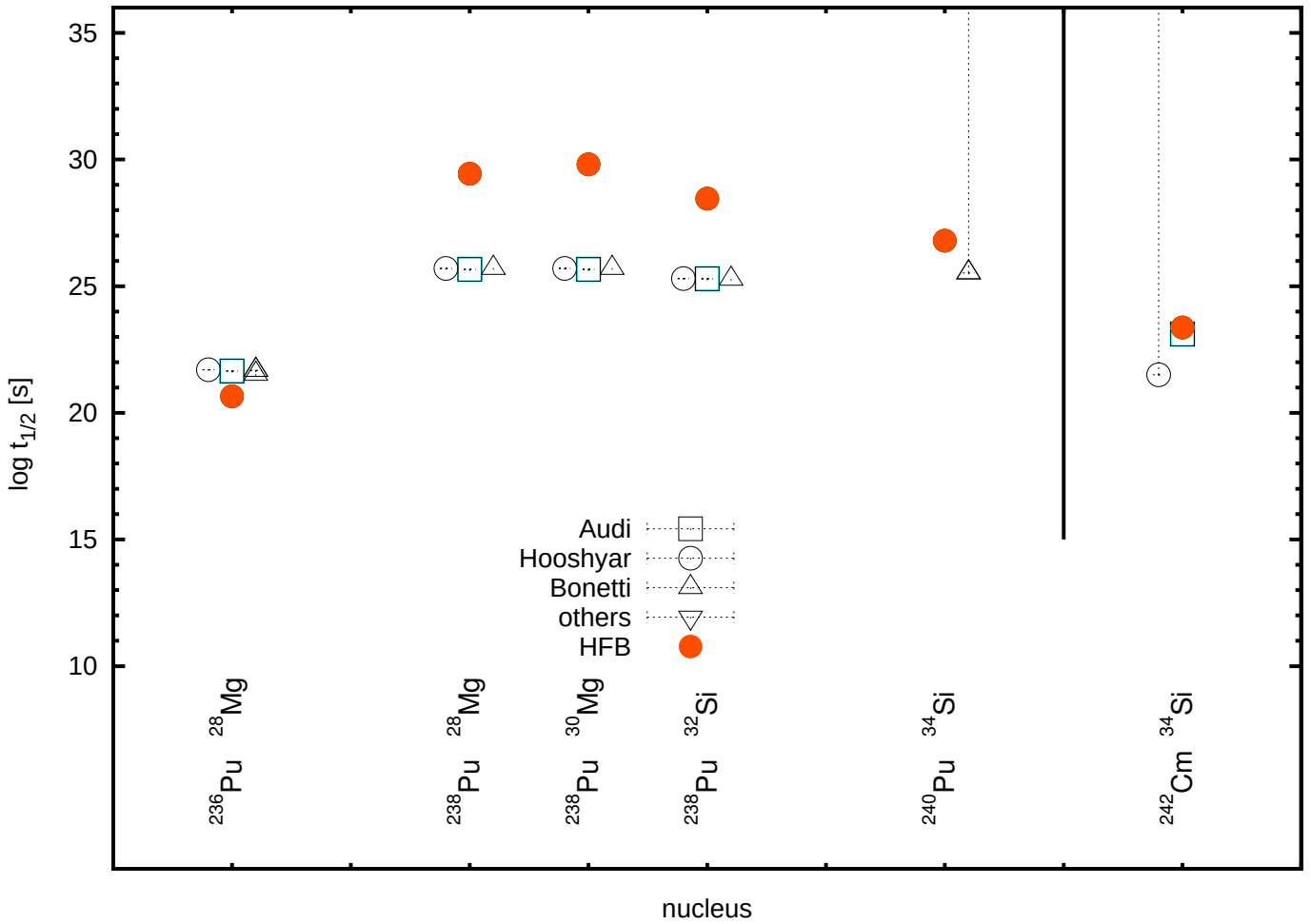

Podsumowanie

- Przebadane została emisja klastrów z jąder aktynowców w samozgodnym modelu HFB z siłami D1S Gogny

Podsumowanie

- Przebadane została emisja klastrów z jąder aktynowców w samozgodnym modelu HFB z siłami D1S Gogny
- Znaleziono ścieżki rozpadu prowadzące emisji klastrów

Podsumowanie

- Przebadane została emisja klastrów z jąder aktynowców w samozgodnym modelu HFB z siłami D1S Gogny
- Znaleziono ścieżki rozpadu prowadzące emisji klastrów
- Wyznaczono masy klastrów

Podsumowanie

- Przebadane została emisja klastrów z jąder aktynowców w samozgodnym modelu HFB z siłami D1S Gogny
- Znaleziono ścieżki rozpadu prowadzące emisji klastrów
- Wyznaczono masy klastrów
- Czasy życia są w rozsądnej zgodności z danymi doświadczalnymi